

# Predictive risk estimation for the Expectation Maximization algorithm with Poisson data

Paolo Massa and Federico Benvenuto

Dipartimento di Matematica, Università di Genova, via Dodecaneso 35, 16146  
Genova, Italy

E-mail: [massa.p@dima.unige.it](mailto:massa.p@dima.unige.it), [benvenuto@dima.unige.it](mailto:benvenuto@dima.unige.it)

September 2020

**Abstract.** In this work, we introduce a novel estimator of the predictive risk with Poisson data, when the loss function is the Kullback-Leibler divergence, in order to define a regularization parameter's choice rule for the Expectation Maximization (EM) algorithm. To this aim, we prove a Poisson counterpart of the Stein's Lemma for Gaussian variables, and from this result we derive the proposed estimator showing its analogies with the well-known Stein's Unbiased Risk Estimator valid for a quadratic loss. We prove that the proposed estimator is asymptotically unbiased with increasing number of measured counts, under certain mild conditions on the regularization method. We show that these conditions are satisfied by the EM algorithm and then we apply this estimator to select its optimal reconstruction. We present some numerical tests in the case of image deconvolution, comparing the performances of the proposed estimator with other methods available in the literature, both in the inverse crime and non-inverse crime setting.

*Keywords:* Predictive risk, SURE-type estimator, Expectation Maximization, Poisson data, Kullback-Leibler divergence, image deconvolution

## 1. Introduction

The Expectation Maximization (EM) algorithm is a general iterative strategy proposed in [19] to compute the Maximum Likelihood (ML) solution of a given estimation problem. EM has been widely applied to Poisson inverse problems, i.e. when measurements are corrupted by Poisson noise: examples arise in medical imaging, astronomical imaging, microscopy and whenever data are collected by means of a counting process [11, 22, 37, 38]. In the special case of deconvolution, it was known as Richardson-Lucy algorithm [28, 35] before the formalization given in [19]. It is well known that the EM algorithm for Poisson data converges to the ML solution which is an unreliable solution of the problem as it is corrupted by noise amplification due to the ill-posedness of the problem. Nonetheless, at the beginning of the EM iterative

process the approximated solutions improve, so that finding the optimal number of iterates, i.e. when the algorithm starts diverging from the exact solution of the inverse problem, is a long standing problem which is of great interest for a number of studies. Such a property is widely known as semiconvergence, or sometimes authors refer to it as self-regularization [30]. In [34] authors have theoretically proven the semiconvergent behaviour of the EM algorithm for noisy data, under some mild assumptions.

Among the many different strategies proposed to stop the EM algorithm for Poisson data, (see e.g. [7, 12, 15, 22, 26, 30] and references therein), in this work we focus on rules based on predictive risk minimization, that has recently gained some attention in the Gaussian framework [3, 6, 18, 25, 27]. The predictive risk is the expectation of the loss function between the the data and the prediction and, in the case of Poisson data, the loss function is the Kullback-Leibler (KL) divergence. To the best of our knowledge, only two strategies have been proposed in the literature to estimate the predictive risk in the case of Poisson inverse problems, each of which relying on a different estimation of the risk function. The first approach was proposed in [36] and it introduces an approximation of the predictive risk based on the Taylor expansion of the KL divergence, without proving its convergence. The second approach has been more recently proposed in [17] and it exploits a statistical estimator valid for the entire class of the generalised linear models (see equations (2.3) and (2.10) in [23]), obtaining an estimator of the predictive risk in the case of Poisson data with an unknown but constant bias, named PUKLA for Poisson Unbiased KL Analysis. The striking fact is that, although the connection between inverse problems and statistical estimation has been well established (see e.g. [21]), it took about forty years before this result was applied to an inverse problem. Nonetheless, this estimator cannot be straightforwardly applied to large sized data due to its computational complexity. In order to overcome this problem, in [17] the author proposed an approximation of PUKLA which relies on a combination of a Taylor expansion and a Monte-Carlo integration (see equation (6.2) in [17]). Also in this case, convergence and statistical properties of this approximation have not been investigated.

In this work, we introduce a novel estimator of the predictive risk with Poisson data, proving that it is asymptotically unbiased when used to choose the optimal number of iterations of the EM algorithm. In order to do this, we state and prove a more general result, a Poisson counterpart of the Stein's Lemma for Gaussian variables [39]. Analogously to the well-known Stein's Unbiased Risk Estimator (SURE), the proposed predictive risk estimator is composed by three parts: the first and the second part of the estimator represent the bias and the variance, respectively, while the third term is the negative asymptotic variance of the estimator. In line with the Gaussian case, the bias term is given by the empirical loss function, whereas the variance term involves the derivative of the influence (or smoothing) operator and the third term is constant. The actual difference between the two decomposition is that in the Poisson case a fourth term exists and, under some regularity assumptions, it tends to zero with increasing number of counts, making this estimator asymptotically unbiased. Operationally, the idea is

then to select the iterate of the EM algorithm when this function takes the minimum, i.e. in terms of an estimation of the bias-variance trade-off. However, we show with some numerical tests in the case of image deconvolution that the performances of all these predictive risk estimators are quite similar: the main advantage of the one proposed in this work is its complete theoretical justification. Indeed, this analysis shed some light also about the above mentioned approximations of the KL based risk (see [17, 36]). The comparison with the Gaussian case becomes straightforward and it is a reference point to identify the role of the terms of the existing estimates. Moreover, it becomes clear that the statistical convergence of these estimators is not guaranteed as it depends on some regularity conditions of the regularization method. Finally, such conditions concern the mathematical properties of the regularization method and they can be verified in advance.

The paper is organised as follows. In section 2 we describe the mathematical formulation of an inverse problem with Poisson data and the EM algorithm viewed as a one-parameter family of estimators. In section 3 we introduce the risk definition and we give the main results of the paper: the asymptotic Stein's Lemma for Poisson variables and the Poisson Asymptotically Unbiased KL risk estimator. Then, in section 4 we prove that the EM algorithm satisfies the conditions under which the proposed predictive risk estimator computed along the EM iterates is asymptotically unbiased. In section 5 we show some numerical tests in the case of image deconvolution, comparing the use of predictive risk estimators and the Poisson discrepancy principle [12]. Section 6 is devoted to conclusions. Proofs of the main results are contained in the Appendix.

## 2. Mathematical formulation

The aim of an ill-posed inverse problem in a semi-discrete setting [13, 34] is to estimate a function  $u^* \in L^2(\mathbb{R}^d)$ , representing an emission density, having random noisy measurements  $Y_1, \dots, Y_M$  of the value of  $M$  linear functionals that can be thought as the components of  $Au^*$ , where  $A: L^2(\mathbb{R}^d) \rightarrow \mathbb{R}^M$  is defined by

$$(Au)_i = \int_{\Omega} u(s)h_i(s) ds \quad , \quad \forall u \in L^2(\mathbb{R}^d) \quad \forall i \in \{1, \dots, M\} \quad (1)$$

with  $\Omega \subseteq \mathbb{R}^d$  a compact set and  $h_i \in L^\infty(\Omega)$ . Typically, the dimension  $d$  is equal to 2 or 3. In the case of Poisson measurements, the additional hypothesis is that

$$Y = (Y_1, \dots, Y_M) \sim \mathcal{P}(Au^* + b) \quad (2)$$

where  $\mathcal{P}(\lambda)$  is the Poisson distribution of parameter  $\lambda$  with independent components and  $b = (b_1, \dots, b_M)$  is a vector whose components  $b_i > 0$  are the mean values of the detected background emission. In applications, such as microscopy or astronomy, equation (1) represents the forward linear operator describing the signal formation by means of the instrument acquisition system: in this case  $\Omega$  is the field of view of the imaging system and  $h_i$  is the transmission function describing the probability that a photon, coming out from the point  $s$ , reaches the  $i$ -th detector. Moreover, the number of counts registered

by the  $M$  detectors is a realization of  $Y_1, \dots, Y_M$ . Finally, the function  $u^* \geq 0$  satisfies the non-negativity hypothesis as it represents the intensity of a photon emission.

In practical applications a discretisation of (1) is required; this means that the domain  $\Omega$  is partitioned into  $N$  cells with the same area (or volume)  $\Delta s$ . Equation (1) can be rewritten as

$$(Au)_i = \sum_{j=1}^N x_j h_{i,j} \Delta s, \quad (3)$$

where  $x_j$  and  $h_{i,j}$  are the mean values in the  $j$ -th cell of the functions  $u$  and  $h_i$  respectively. The unknown function  $u^*$  becomes then a vector in  $\mathbb{R}^N$  and the forward linear operator a matrix which we denote with  $x^*$  and  $H \in \mathbb{R}^{M \times N}$  respectively; in particular the entries of  $H$  are given by

$$H_{ij} = h_{i,j} \Delta s. \quad (4)$$

As measurements are counting processes drawn from a Poisson random variable  $Y$  with independent components and mean value  $\lambda = Hx^* + b \in \mathbb{R}_{++}^M$ , we can assume that the vector of data recorded is a realization  $y \in \mathbb{R}_+^M$ . Then, the problem of determining the object from the measurements is the discrete inverse problem given by the equation

$$y = Hx + b, \quad (5)$$

where  $x = (x_1, \dots, x_M)$ . We assume  $H_{ij} > 0$  for all  $i, j$  as in [34]; we point out that this assumption, very restrictive from a theoretical view point, is not a limitation in practice as we can always numerically approximate a matrix with non-negative components with another one with arbitrarily small positive entries. For example, denoising applications, for which  $H = I$  and  $b = 0$ , can be considered as a limiting case of this hypothesis.

The probability of observing a data  $y$  corresponding to an object  $x$  is given by

$$p(y; x) := \prod_{i=1}^M \frac{e^{-(Hx+b)_i} (Hx+b)_i^{y_i}}{y_i!}, \quad (6)$$

therefore, determining the unknown corresponds to estimating the parameter of a Poisson variable. The ML approach consists in finding the value of the parameter  $x$  for which the log-likelihood function  $\log L_y(x) := \log(p(y; x))$  takes its maximum, i.e. in solving

$$\arg \max_{x \in \mathbb{R}_+^M} \left\{ \log L_y(x) = \sum_{i=1}^M -(Hx+b)_i + y_i \log(Hx+b)_i - \log(y_i!) \right\}. \quad (7)$$

It is worth noticing that, by changing the sign of the objective function and by subtracting terms that are constant with respect to  $x$ , it can be readily shown that problem (7) is equivalent to

$$\arg \min_{x \in \mathbb{R}_+^M} D_{\text{KL}}(y, Hx + b), \quad (8)$$

where  $D_{\text{KL}}$  is the Kullback-Leibler divergence [14] defined by

$$D_{\text{KL}}(u, v) := \sum_{i=1}^M u_i \log \frac{u_i}{v_i} + v_i - u_i \quad (9)$$

for all  $u \in \mathbb{R}_+^M$  and for all  $v \in \mathbb{R}_{++}^M$ . When data are Poisson distributed, the EM algorithm takes the form

$$x_{k+1} = \psi_y(x_k) \quad (10)$$

where

$$\psi_y(x) := \frac{x}{H^T \mathbf{1}} H^T \left( \frac{y}{Hx + b} \right) . \quad (11)$$

where  $\mathbf{1}$  represents a vector with entries all equal to one and multiplication and division between vectors are meant component-wise. The usual initialisation is  $x_0 = \mathbf{1}$ . This algorithm was presented in [38] as a application of the general EM strategy proposed in [19] to the case of image deconvolution and it is a slight modification of the method introduced by Richardson [35] and Lucy [28] for taking into account the background emission  $b$ . Moreover, examples when the operator  $H$  is space variant arise both in astronomy [8, 29] and biomedicine [31, 37]. Following [2, 5], the  $k$ -th iterate of the EM algorithm can be written in closed form as a function of the data  $y$ . In particular, the function  $R_k: \mathbb{R}_+^M \rightarrow \mathbb{R}_+^M$  such that  $R_k(y) = x_k$ , is

$$R_k(y) := \underbrace{(\psi_y \circ \dots \circ \psi_y)}_{k \text{ times}}(x_0) \quad (12)$$

with  $R_0(y) := x_0$  for all  $y \in \mathbb{R}_+^M$ .

Due to the ill-posedness of the inverse problem (1), the discrete forward operator  $H$  is ill-conditioned and the ML solution is deprived of physical meaning [10]. Moreover, the semiconvergent behaviour of the EM algorithm is a well known property [10, 34]; in particular for  $b = 0$ , it has been recently proved in [32] that the solution of (8) (possibly reached for  $k = +\infty$ ) is composed by a few non-zero components that gives rise to spikes in the reconstructed image. Therefore, the EM algorithm requires regularization in the form of a stopping rule that prevents over-fitting of noisy data.

### 3. Asymptotic Stein's Lemma for Poisson KL risk estimator

To regularize the EM algorithm by early stopping the iterations, several approaches have been investigated in the literature; in particular there exists a class of methods based on the predictive risk estimate [1, 17, 36]. In this paper we follow this strategy, motivated by the considerations below. In the inverse problem (5), the data  $y$  is a realization of the Poisson random variable  $Y$  and the  $k$ -th iterate of the EM algorithm gives rise to an estimator of its mean value  $\lambda$ , defined by

$$\hat{\lambda}_k(Y) := HR_k(Y) + b . \quad (13)$$

The semiconvergent behaviour of the EM algorithm is reflected in the fact that  $D_{\text{KL}}(y, \hat{\lambda}_k(y)) \rightarrow 0$  as  $k \rightarrow +\infty$ ; therefore, as the number of iterations increases, the estimate  $\hat{\lambda}_k(y)$  of  $\lambda$  gets more and more biased towards  $y$ . Actually, we would like to stop the algorithm at the iterate  $k^*$  such that

$$k^* = \arg \min_{k \in \mathbb{N}} D_{\text{KL}}(\lambda, \hat{\lambda}_k(y)) , \quad (14)$$

but the computation of  $D_{\text{KL}}(\lambda, \hat{\lambda}_k(y))$  is unfeasible because it depends on the value of  $\lambda$  which is unknown. The idea is to replace this quantity with its expected value with respect to the random variable  $Y$  and therefore to find the iterate  $k^*$  that satisfies

$$k^* = \arg \min_{k \in \mathbb{N}} \mathbb{E}(D_{\text{KL}}(\lambda, \hat{\lambda}_k(Y))) . \quad (15)$$

We observe that  $\mathbb{E}(D_{\text{KL}}(\lambda, \hat{\lambda}_k(Y)))$  is the risk of the estimator  $\hat{\lambda}_k(Y)$  when the KL divergence is the loss function; from the point of view of the estimator  $R_k(Y)$  of the reconstructed image it is called *predictive risk*. For the sake of clarity, we recall the definition of risk in the statistical framework. It is worth noticing that the definition we adopted is obtained by considering an estimator as decision function [9, 21].

**Definition 3.1 (Risk of an estimator)** *Let  $\theta \in \Theta$  be a parameter of a random variable  $Y$  that takes values in a set  $\mathcal{Y}$  and let  $\hat{\theta}: \mathcal{Y} \rightarrow \mathcal{A}$  be a function such that  $\hat{\theta}(Y)$  is an estimator of  $\theta$ . The risk of the estimator  $\hat{\theta}(Y)$ , computed with respect to the loss function  $L: \Theta \times \mathcal{A} \rightarrow [0, +\infty]$ , is the quantity*

$$r_\theta(\hat{\theta}(Y)) := \mathbb{E}(L(\theta, \hat{\theta}(Y))) . \quad (16)$$

This definition applies to our case by taking  $L$  the KL divergence,  $Y$  a Poisson random variable and  $\theta$  its mean value  $\lambda$ . Moreover, the role of  $\hat{\theta}$  is played at each iteration of the EM algorithm by  $\hat{\lambda}_k$ . Once again one point out that, in order to compute the value of  $\mathbb{E}(D_{\text{KL}}(\lambda, \hat{\lambda}_k(Y)))$ , it is necessary to know  $\lambda$ ; actually, as we will show in the following, it is possible to obtain estimators of  $\mathbb{E}(D_{\text{KL}}(\lambda, \hat{\lambda}_k(Y)))$  that do not depend on  $\lambda$ , therefore we will determine the iterate  $k^*$  by replacing the risk in (15) with an estimator of its.

Unbiased risk estimation has been widely studied in the past decades; in particular, the most famous case is the one concerning normal random variables and the square  $\ell^2$  norm as loss. In [39] Stein proved that, given  $Y \sim \mathcal{N}(\mu, \sigma^2 I)$  an  $M$ -dimensional normal random variable and  $\hat{\mu}(Y)$  an estimator of  $\mu$ , under suitable conditions on  $\hat{\mu}$  it holds true that the risk  $\mathbb{E}(\|\hat{\mu}(Y) - \mu\|^2)$  can be unbiasedly estimated by the Stein's Unbiased Risk Estimator (SURE)

$$\text{SURE}(Y) := \|\hat{\mu}(Y) - Y\|^2 + 2\sigma^2 \nabla \cdot \hat{\mu}(Y) - M\sigma^2 . \quad (17)$$

The derivation of (17) is essentially based on a result, named Stein's Lemma, which states that, for all  $i \in \{1, \dots, M\}$

$$\mathbb{E}((Y_i - \mu_i)f(Y)) = \mathbb{E}(\sigma^2 \partial_i f(Y)) , \quad (18)$$

if  $f: \mathbb{R}^M \rightarrow \mathbb{R}$  satisfies some mild conditions. In the case of an  $M$ -dimensional Poisson random variable  $Y \sim \mathcal{P}(\lambda)$  with independent entries an analogous formulation of (17) was given [17, 23]. If  $\hat{\lambda}(Y)$  is an estimator of  $\lambda$ , then  $\mathbb{E}(\|\hat{\lambda}(Y) - \lambda\|^2)$  can be estimated by the Poisson Unbiased Risk Estimator (PURE)

$$\text{PURE}(Y) := \|\hat{\lambda}(Y)\|^2 - 2Y \cdot \hat{\lambda}_\downarrow(Y) + Y \cdot (Y - 1) , \quad (19)$$

where  $\hat{\lambda}_\downarrow(Y)_i := \hat{\lambda}(Y - e_i)_i$  for all  $i \in \{1, \dots, M\}$  and  $e_i$  is the  $i$ -th element of the canonical basis. As explained in [17], considering the square  $\ell^2$  norm as loss for the

risk of  $\hat{\lambda}$  is not very effective in practice because it does not take into account the heteroscedasticity of the Poisson random variable. Therefore the KL divergence was considered as loss function and it was proved that the risk  $\mathbb{E}(D_{\text{KL}}(\lambda, \hat{\lambda}(Y)))$  can be unbiasedly estimated by the Poisson Unbiased KL Analysis (PUKLA) estimator

$$\text{PUKLA}(Y) := \|\hat{\lambda}(Y)\|_1 - Y \cdot \log \hat{\lambda}_\downarrow(Y), \quad (20)$$

where the logarithm is applied component-wise. The computation of PUKLA is very expensive in practice as it requires  $M$  times the evaluation of  $\hat{\lambda}$  (in the image reconstruction problem of interest it means that  $M$  reconstructions are needed). Moreover, from a theoretical point of view, it requires that the function  $\hat{\lambda}$  is defined on  $[-1, +\infty[^M$  and this is not the case for  $\hat{\lambda}_k$ . Finally, the PUKLA estimator is not truly unbiased: it does not provide an absolute quantification of the risk as it is defined up to an additive constant. In [36] the authors introduce a different estimator of the risk with KL loss, defined by

$$\text{REKL}(Y) := \sum_{i=1}^M \hat{\lambda}(Y)_i - Y_i \log \hat{\lambda}(Y)_i + \frac{MY_i \eta_i}{2\varepsilon \|\eta\|^2} \left( \log \hat{\lambda}(Y + \varepsilon \eta)_i - \log \hat{\lambda}(Y - \varepsilon \eta)_i \right) \quad (21)$$

where  $\eta \sim \mathcal{N}(0, I)$  is an  $M$ -dimensional normal random variable and  $\varepsilon$  is a small positive constant. This estimator is derived from a Taylor expansion of the KL divergence and the second term comes from a Monte-Carlo approximation involving the trace of a Jacobian matrix. Although very effective in practice, it has no rigorous theoretical justification, as it is not proven that the Taylor's remainder is negligible, at least in some asymptotic sense. Moreover, as the PUKLA estimator, it is defined up to an unknown additive constant. Other estimators of the predictive risk, based on the application of the Generalized Cross Validation (GCV) and the Unbiased Predictive Risk Estimator (UPRE) to a Gaussian approximation of the KL divergence, have been presented in [1]

In this section we propose a new estimator of  $\mathbb{E}(D_{\text{KL}}(\lambda, \hat{\lambda}(Y)))$  that is analogous to SURE (17) when Poisson data are considered. We also give some mild conditions under which the proposed estimator is unbiased in an asymptotic regime, i.e. when every component of the mean  $\lambda$  is sufficiently large. Moreover, differently from the previous ones, the proposed estimator is not defined up to an additive constant, but it estimates the actual value of the risk. First of all we give an asymptotic Stein's Lemma for Poisson random variables. The proof of this result is given in the Appendix.

**Lemma 3.1 (Asymptotic Stein's Lemma for Poisson random variables)** *Let  $Y$  be a multivariate Poisson random variable with mean value  $\lambda \in \mathbb{R}_{++}^M$  and independent components,  $\mathcal{C} \subset \mathbb{R}_{++}^M$  a closed convex cone containing  $\lambda$  and  $f: \mathbb{R}_{++}^M \rightarrow \mathbb{R}$  a function such that:*

- (i)  $\mathbb{E}(|Y_i f(Y)|) < +\infty$  for all  $i \in \{1, \dots, M\}$ ;
- (ii)  $f \in C^2(\mathbb{R}_+^M)$ ;
- (iii) for all  $j \in \{1, \dots, M\}$  there exist  $c_j, \varepsilon_j > 0$  such that

$$|\partial_j f(y)| \leq \frac{c_j}{\|y\| + \varepsilon_j} \quad (22)$$

for all  $y \in \mathbb{R}_+^M$ ;

(iv) for all  $k, l \in \{1, \dots, M\}$  there exist  $\varepsilon_{k,l}, c_{k,l} > 0$  such that

$$|\partial_k \partial_l f(y)| \leq \frac{c_{k,l}}{\|y\|^2 + \varepsilon_{k,l}} \quad (23)$$

for all  $y \in \mathbb{R}_+^M$ .

Then, for all  $i \in \{1, \dots, M\}$

$$\mathbb{E}((Y_i - \lambda_i) f(Y)) = \mathbb{E}(Y_i \partial_i f(Y)) + O(\|\lambda\|^{-1/2}) \quad (24)$$

as  $\|\lambda\| \rightarrow +\infty$  in  $\mathcal{C}$ .

The analogy between (18) and (24) is in the fact that the left-hand side is the same, while in the right-hand side the term  $\sigma^2$ , which is the known variance of  $Y_i$  in the normal case, is replaced with  $Y_i$  that is an unbiased estimator of the variance in the Poisson case. We point out that the introduction of the cone  $\mathcal{C}$  in (24) is just a technical fact needed by the proof in order to have a result which is uniform in the variable  $\lambda$  while keeping the property that every component of  $\lambda$  tends to  $+\infty$  as the norm  $\|\lambda\|$  does.

Lemma 3.1 allow us to derive an estimator of the risk with KL loss for Poisson variates. The proof is contained in the Appendix.

**Theorem 3.1 (Poisson Asymptotically Unbiased KL risk estimator)** *Let  $Y$  be a multivariate Poisson random variable with mean value  $\lambda \in \mathbb{R}_{++}^M$  and independent components and let  $\hat{\lambda}(Y)$  be an estimator of  $\lambda$  taking values in  $\mathbb{R}_{++}^M$ . Let us assume that every component of the function  $\log \hat{\lambda}: \mathbb{R}_+^M \rightarrow \mathbb{R}^M$  satisfies the hypothesis (i)-(iv) of Lemma 3.1. Then,*

$$\text{PAUKL}(Y) := D_{\text{KL}}(Y, \hat{\lambda}(Y)) + (Y \nabla) \cdot \log \hat{\lambda}(Y) - \frac{M}{2}, \quad (25)$$

where  $Y \nabla := (Y_1 \partial_1, \dots, Y_M \partial_M)$ , is an asymptotically unbiased estimator of the risk  $\mathbb{E}(D_{\text{KL}}(\lambda, \hat{\lambda}(Y)))$  in the sense that, if  $\mathcal{C} \subset \mathbb{R}_{++}^M$  is a closed cone containing  $\lambda$ , we have

$$\mathbb{E}(D_{\text{KL}}(\lambda, \hat{\lambda}(Y))) = \mathbb{E}(\text{PAUKL}(Y)) + O(\|\lambda\|^{-1/2}). \quad (26)$$

as  $\|\lambda\| \rightarrow +\infty$  in  $\mathcal{C}$ .

We remark the similarities between SURE and PAUKL: in both the estimators the first term represents the discrepancy between the observed data and the currently estimated mean value, the second term is related to the divergence of the estimator and the third term is the negative expected value between the random variable  $Y$  and its mean value. From a practical point of view, using (25) instead of (20) for estimating the KL risk can be very convenient as the computation of (25) does not require multiple evaluations of  $\hat{\lambda}$ ; on the other hand, if the analytical expression of  $(Y \nabla) \log \hat{\lambda}$  is not available or in the case it is recursively defined as in the case of image reconstruction by means of the EM algorithm, the computation of this quantity can be very expensive or even unfeasible. We will show in section 5 how to obtain an accurate estimate of  $(Y \nabla) \cdot \log \hat{\lambda}$  with a Monte-Carlo method.



#### 4. Predictive risk for the EM algorithm for Poisson data

In this section we prove that it is possible to use (25) for estimating the predictive risk of the  $k$ -th iterate of the EM algorithm; in particular, we will show that  $\log \hat{\lambda}_k$  satisfies the hypothesis of Theorem 3.1. Basically, what is needed is that every component of  $\log \hat{\lambda}_k$  is smooth and that its first and second order partial derivatives are bounded by a suitable function that decays sufficiently fast at infinity. We will prove that these requirements are satisfied thanks to the fact every component of  $R_k$  defined in (12) is a rational function of the data  $y$ , in which the difference between the degrees of the polynomials at numerator and denominator is 1.

In the following we will define *homogeneous polynomial* of degree  $n$  a polynomial  $p^{(n)}$  of the form

$$p^{(n)}(y) = \sum_{\alpha \in S(n)} c_{\alpha} y_1^{\alpha_1} \cdots y_M^{\alpha_M} \quad (27)$$

where  $S(n) := \{\alpha \in \mathbb{N}^M : \alpha_1 + \dots + \alpha_M = n\}$  and  $c_{\alpha} \in \mathbb{R}$ ; we will also call  $p^{(n)}$  *complete* if  $c_{\alpha} \neq 0$  for all  $\alpha \in S(n)$ .

**Proposition 4.1** *The  $k$ -th iterate of the EM algorithm for Poisson data is a rational function, i.e. for all  $j \in \{1, \dots, N\}$  we can write*

$$(R_k(y))_j = \frac{p_{k,j}^{(d+1)}(y) + \dots + p_{k,j}^{(0)}}{q_{k,j}^{(d)}(y) + \dots + q_{k,j}^{(0)}} \quad (28)$$

with  $d \in \mathbb{N}$ , where:

- (i)  $p_{k,j}^{(n)}$  and  $q_{k,j}^{(m)}$  are homogeneous polynomials with nonnegative coefficients for all  $n \in \{0, \dots, d+1\}$  and for all  $m \in \{0, \dots, d\}$ ;
- (ii)  $p_{k,j}^{(d+1)}$ ,  $q_{k,j}^{(d)}$  are complete and  $q_{k,j}^{(0)} > 0$ .

Thanks to this result, it is possible to show that  $\log \hat{\lambda}_k$  satisfies the hypothesis of Theorem 3.1.

**Proposition 4.2** *Let us fix the  $k$ -th iterate of the EM algorithm. For all  $i \in \{1, \dots, M\}$  the following hold true:*

- (i)  $(\log \hat{\lambda}_k)_i \in C^{\infty}(\mathbb{R}_+^M)$ ;
- (ii) for all  $j \in \{1, \dots, M\}$  there exist  $c_j, \varepsilon_j > 0$  such that

$$|\partial_j (\log \hat{\lambda}_k(y))_i| \leq \frac{c_j}{\|y\| + \varepsilon_j} \quad (29)$$

for all  $y \in \mathbb{R}_+^M$ ;

- (iii) for all  $l, r \in \{1, \dots, M\}$  there exist  $\varepsilon_{l,r}, c_{l,r} > 0$  such that

$$\left| \partial_l \partial_r (\log \hat{\lambda}_k(y))_i \right| \leq \frac{c_{l,r}}{\|y\|^2 + \varepsilon_{l,r}} \quad (30)$$

for all  $y \in \mathbb{R}_+^M$ .

The proofs are given in the Appendix.

## 5. Numerical simulations

We perform our numerical tests in the case of deconvolution of astronomical images. In particular, we report the results obtained on two  $256 \times 256$  images from the Hubble Space Telescope: the nebula NGC7027 (<http://www.oasis.unimore.it/site/home/software.html>) and the Horsehead Nebula (<http://www.astropy.org/astropy-data>). At every iteration of EM we compute the PAUKL estimator of the predictive risk and we stop the algorithm once its minimum is reached. We compare the performances of PAUKL with the ones of PUKLA, REKL and of the discrepancy principle for Poisson data.

For applying the PAUKL estimator we need to compute the term  $(y\nabla) \cdot \log \hat{\lambda}_k(y)$  in (25). In the case of the EM algorithm, it is possible to obtain a recursive expression of this quantity that at every iteration depends only on the previous one, but the computational burden of the operations required is too high in practice. In our experiments we decide to approximate it by using a Monte-Carlo method derived in [33]. Exploiting the fact that

$$(y\nabla) \cdot \log \hat{\lambda}_k(y) = \lim_{\varepsilon \rightarrow 0^+} \mathbb{E} \left( (y\eta) \cdot \left( \frac{\log \hat{\lambda}_k(y + \varepsilon\eta) - \log \hat{\lambda}_k(y)}{\varepsilon} \right) \right) \quad (31)$$

where  $\eta \sim \mathcal{N}(0, I)$  is an  $M$ -dimensional normal random variable and the mean value is computed with respect to  $\eta$ , we estimate

$$(y\nabla) \cdot \log \hat{\lambda}_k(y) \approx (y\eta) \cdot \left( \frac{\log \hat{\lambda}_k(y + \varepsilon\eta) - \log \hat{\lambda}_k(y)}{\varepsilon} \right) \quad (32)$$

with  $\varepsilon$  fixed to  $10^{-3}$ . This estimation has the computational cost of two reconstructions and it is therefore very efficient on large-scale problems. Similarly, in order to be able to apply the PUKLA estimator without performing  $M$  reconstructions, we decide to use the approximation given by equation (6.2) in [17]:

$$y \cdot \log \hat{\lambda}_{k\downarrow}(y) \approx y \cdot \log \hat{\lambda}_k(y) - (y\zeta) \cdot (\nabla \log \hat{\lambda}_k(y)\zeta) \quad (33)$$

where  $\zeta = (\zeta_1, \dots, \zeta_M)$  and  $\zeta_i$  is a Bernoulli variable with parameter  $p = 1/2$  taking values in  $\{-1, 1\}$ . This equation reveals an idea of (25), but this is the first time that a rigorous proof is given. Following what done in (32), we use the difference quotient to approximate the derivative, obtaining

$$y \cdot \log \hat{\lambda}_{k\downarrow}(y) \approx y \cdot \log \hat{\lambda}_k(y) - (y\zeta) \cdot \left( \frac{\log \hat{\lambda}_k(y + \varepsilon\zeta) - \log \hat{\lambda}_k(y)}{\varepsilon} \right) \quad (34)$$

with  $\varepsilon$  fixed to  $10^{-3}$ . Thanks to these considerations, it is possible to compute an approximated version of PUKLA by performing just two reconstructions instead of  $M$ .

We point out that in the deconvolution inverse problem the entries of the matrix operator  $H$  do not satisfy the hypothesis to be strictly positive. This requirement is heavily used to prove the theoretical results, but in our experience we noticed that it is not necessary in practice.

### 5.1. Inverse crime setting

We generate the data  $y$  as a realization of a Poisson variable  $Y \sim \mathcal{P}(Hx^* + b)$ , where  $x^*$  is the image of the nebula,  $H$  is the convolution operator with a Gaussian Point Spread Function (PSF) with a standard deviation  $\sigma = 3$  expressed in pixel unit, and  $b$  is a constant background whose components are equal to 100 for the nebula NGC7027 and equal to 10 for the Horse Head nebula. For both images we consider three different levels of statistic, i.e. we rescale  $x^*$  so that the sum of the pixel values is equal to  $10^7$  in the low statistic case,  $10^8$  in the medium statistic case and  $10^9$  in the high statistic case.

We reconstruct the images with the EM algorithm from a single realization of the data  $y$  for each level of statistic. At every iteration  $k$  of EM we compute the estimators of the predictive risk (PAUKL, REKL and PUKLA) and the discrepancy with the KL divergence, i.e.

$$d_{\text{KL}}(k, y) := D_{\text{KL}}(y, \hat{\lambda}_k(y)) . \quad (35)$$

We stop the iterations when the minimum of the estimators of the risk is reached or when the Poisson discrepancy principle is satisfied, that is once

$$d_{\text{KL}}(k, y) < \frac{M}{2} . \quad (36)$$

For the sake of brevity, we report the reconstructions obtained just in the low statistic case for the nebula NGC7027 (see figure 1) and in the high statistic case for the Horse Head nebula (see figure 2). We do not show the images obtained with PUKLA and REKL as they are too similar to the ones obtained with PAUKL.

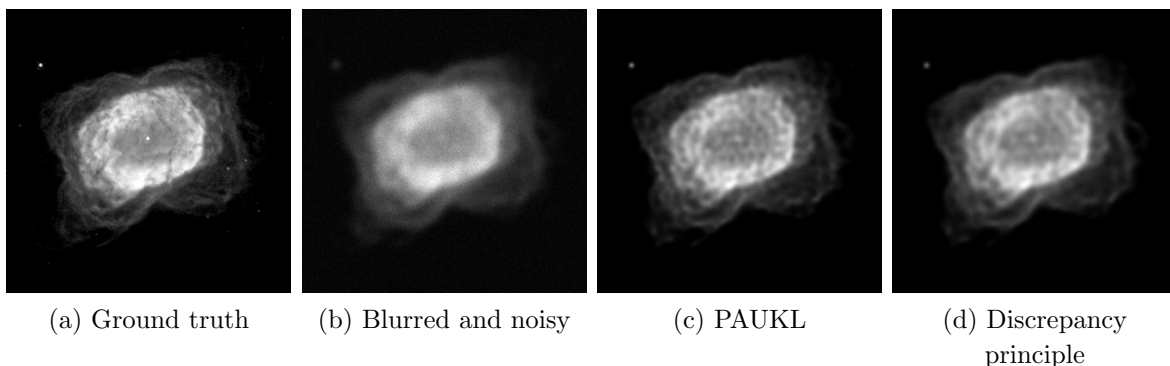


**Figure 1.** Reconstructions of the nebula NGC7027 in the low statistic case (total flux equal to  $10^7$ ). From left to right: ground truth image, blurred and noisy data, reconstruction obtained with PAUKL and reconstruction obtained with the Poisson discrepancy principle.

In order to compare the different estimates of the predictive risk, we perform reconstructions for 25 realizations of Poisson noise  $y_1, \dots, y_{25}$ . Defined the Predictive Error (PE) at every iteration as

$$\text{PE}(k, \lambda, y) := D_{\text{KL}}(\lambda, \hat{\lambda}_k(y)) , \quad (37)$$

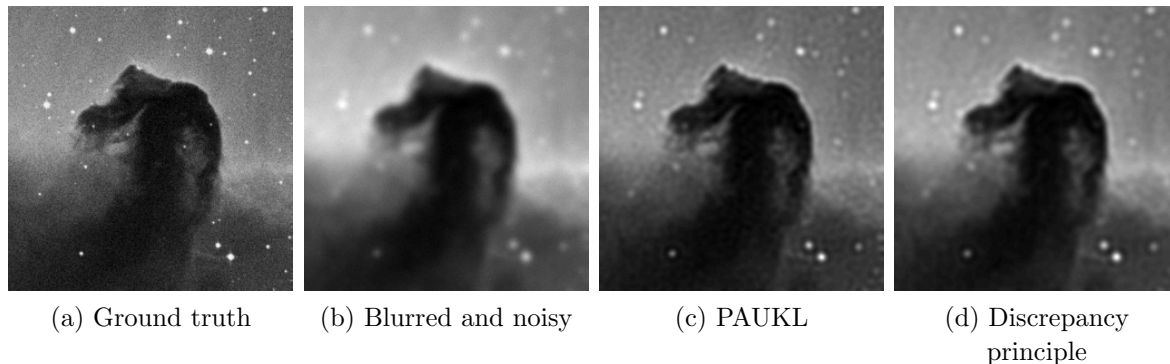


**Figure 2.** Reconstructions of the Horse Head nebula in the high statistic case (total flux equal to  $10^9$ ). From left to right: ground truth image, blurred and noisy data, reconstruction obtained with PAUKL and reconstruction obtained with the Poisson discrepancy principle.

we compute what we call Sample Predictive Risk (SPR), i.e.

$$\text{SPR}(k, \lambda) := \frac{1}{n} \sum_{i=1}^n \text{PE}(k, \lambda, y_i) . \quad (38)$$

where  $n = 25$ . This quantity represents the most accurate estimate of the predictive risk that we can have in the simulation tests, as an analytical computation of  $\mathbb{E}(D_{\text{KL}}(\lambda, \hat{\lambda}_k(Y)))$  is not feasible even if  $\lambda$  is known. At each iteration we also calculate

$$\text{PDP}(k, y) := \left| d_{\text{KL}}(k, y) - \frac{M}{2} \right| . \quad (39)$$

This quantity is related to the Poisson discrepancy principle as the minimum of PDP is reached at the iteration at which the principle is satisfied. We report in figure 3(a) the SPR and the mean values of PAUKL, REKL, PUKLA and PDP on 25 realizations of the data for the nebula NGC7027 in the medium statistic case. Figure 3(b) contains instead a zoom of figure 3(a) in correspondence to the minimum of the estimators of the predictive risk in order to make the differences between them more visible. We point out that the quantities reported in figures 3(a) and 3(b) are not directly comparable and therefore each one of them has been translated by adding a constant value.

We have already remarked that PAUKL, differently from REKL and PUKLA, is able to approximate the actual value of the predictive risk. In order to assess this ability, in figure 3(c) we show the SPR and the mean value of PAUKL on 25 realizations of Poisson noise for the image of nebula NGC7027 in the medium statistic case. The shaded area is in correspondence to the standard deviation of the proposed estimator.

We empirically study the problem to understand if the minimum predictive risk is a valid criterion for obtaining good reconstructions. Denoted  $\text{err}_{\ell^2}$  and  $\text{err}_{\text{KL}}$  the reconstruction errors at every iteration computed with the  $\ell^2$  norm and with the KL divergence respectively, i.e.

$$\text{err}_{\ell^2}(k, x^*, y) := \|x^* - R_k(y)\| , \quad \text{err}_{\text{KL}}(k, x^*, y) := D_{\text{KL}}(x^*, R_k(y)) , \quad (40)$$

we compute the empirical risks

$$\text{ER}_{\ell^2}(k, x^*) := \frac{1}{n} \sum_{i=1}^n \text{err}_{\ell^2}(k, x^*, y_i), \quad \text{ER}_{\text{KL}}(k, x^*) := \frac{1}{n} \sum_{i=1}^n \text{err}_{\text{KL}}(k, x^*, y_i), \quad (41)$$

with  $n = 25$ , in the case of nebula NGC7027 with medium statistic. We plot them together with the SPR in figure 3(d). Again, a translation is applied in order to make the lines comparable.

Finally, we perform 25 reconstructions with the EM algorithm, for both images and for each level of statistic, from different realization of Poisson noise in the data. For each reconstruction we compute the number of iterations at which the minimum of PE, PAUKL, PUKLA, REKL, PDP,  $\text{err}_{\text{KL}}$  and  $\text{err}_{\ell^2}$  is reached. We report in table 1 the mean value and the standard deviation of this number calculated on the 25 reconstructions.

Statistic	PE	PAUKL	PUKLA	REKL	PDP	$\text{err}_{\text{KL}}$	$\text{err}_{\ell^2}$
<b>NGC7027</b>							
Low	76 <sub>(±4)</sub>	78 <sub>(±4)</sub>	78 <sub>(±5)</sub>	79 <sub>(±6)</sub>	31 <sub>(±6)</sub>	89 <sub>(±3)</sub>	52 <sub>(±3)</sub>
Medium	312 <sub>(±13)</sub>	303 <sub>(±24)</sub>	306 <sub>(±28)</sub>	303 <sub>(±29)</sub>	82 <sub>(±10)</sub>	402 <sub>(±14)</sub>	255 <sub>(±11)</sub>
High	2229 <sub>(±121)</sub>	2311 <sub>(±223)</sub>	2308 <sub>(±245)</sub>	2329 <sub>(±358)</sub>	373 <sub>(±41)</sub>	2836 <sub>(±122)</sub>	1612 <sub>(±92)</sub>
<b>Horse Head</b>							
Low	7 <sub>(±1)</sub>	7 <sub>(±1)</sub>	6 <sub>(±1)</sub>	7 <sub>(±0)</sub>	4 <sub>(±0)</sub>	5 <sub>(±0)</sub>	6 <sub>(±0)</sub>
Medium	33 <sub>(±1)</sub>	32 <sub>(±2)</sub>	32 <sub>(±2)</sub>	32 <sub>(±2)</sub>	10 <sub>(±1)</sub>	33 <sub>(±1)</sub>	38 <sub>(±1)</sub>
High	185 <sub>(±11)</sub>	186 <sub>(±10)</sub>	188 <sub>(±11)</sub>	186 <sub>(±13)</sub>	44 <sub>(±3)</sub>	213 <sub>(±9)</sub>	245 <sub>(±9)</sub>

**Table 1.** Comparison between the number of iterations that minimizes the PE, the estimators of the predictive risk (PAUKL, PUKLA and REKL), the PDP and the reconstruction errors ( $\text{err}_{\text{KL}}$  and  $\text{err}_{\ell^2}$ ). We report the mean value and the standard deviation corresponding to 25 Poisson noise realizations of the data.

From the numerical tests it is evident that the performances of the three estimators of the risk, i.e. PAUKL, REKL and PUKLA, are very similar as every one of them is able to give an accurate estimate of the SPR without the knowledge of  $\lambda$  (see figures 3(a), 3(b)). The advantage of the proposed estimator with respect to REKL and PUKLA is that it is not biased with a constant and unknown quantity, but it gives an absolute quantification of the predictive risk. This is shown in figure 3(c) where one can notice that the SPR falls inside the standard deviation of PAUKL. Moreover, we can observe that the stopping rule based on the Poisson discrepancy principle is almost everywhere too much conservative with respect to the rules based on the predictive risk. This fact results in figures 1 and 2, where the reconstructions obtained with the discrepancy principle appear too much regularized. It is also evident in table 1, where the mean value of the number of the iterations at which the Poisson discrepancy principle is satisfied is much lower than the mean values of the number of iterations that correspond to the minimum of the quantities  $\text{err}_{\text{KL}}$  and  $\text{err}_{\ell^2}$ . On the other hand, the discrepancy principle seems to be more stable as a stopping rule as the standard deviation of the

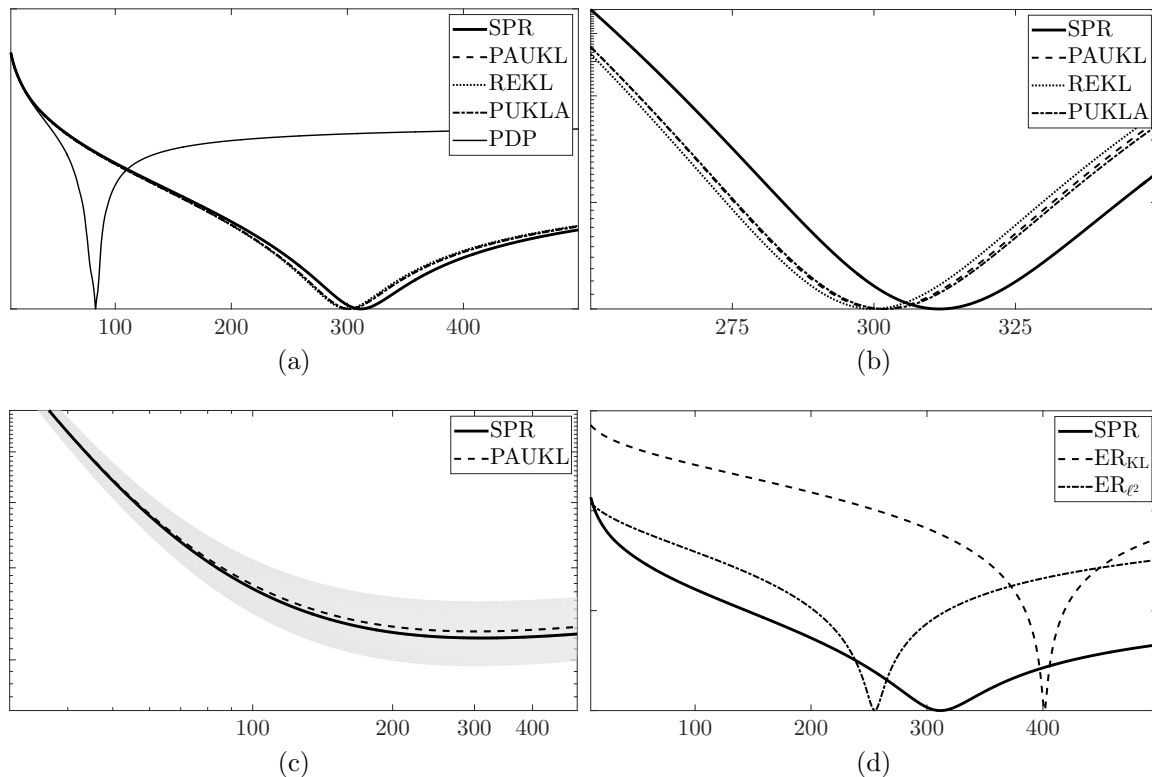


**Figure 3.** Results obtained on the image of nebula NGC7027 in the medium statistic case. Figure (a): comparison between the SPR and the mean values of PAUKL, REKL, PUKLA and PDP on 25 Poisson noise realizations of the data. Figure (b): zoom of figure (a). Figure (c): comparison between the SPR (solid line) and the mean value PAUKL (dashed line) on 25 realizations of the data. The shaded area corresponds to the standard deviation of PAUKL. Figure (d): comparison between the SPR (solid line) and the empirical risks  $ER_{KL}$  (dashed line) and  $ER_{\ell^2}$  (dot-dashed line). In each figure the number of iterations is reported on the x-axis. Figures (a)-(d) are plotted in logarithmic scale on the y-axis and figure (c) is plotted in logarithmic scale also on the x-axis.

number of iterations at which the PDP is minimized is much lower with respect to the standard deviation of the number of iterations at which the estimators of the risk reach the minimum (see table 1). Finally, despite the ill-posedness of the inverse problem, the predictive risk is an effective rule for stopping the EM algorithm. The order of magnitude of the number of iterations at which  $ER_{KL}$  or  $ER_{\ell^2}$  is minimized is the same of the number of iterations at which the SPR or the estimators of the risk are minimized (see figure 3(d)). Same considerations hold true also for the PE and the reconstruction errors  $err_{KL}$  and  $err_{\ell^2}$  in the case of a single realization of the noise (see table 1). The EM algorithm with Poisson data is slow, therefore even if the iteration selected by a predictive risk stopping rule is not exactly the same as the one that corresponds to the minimum of  $err_{KL}$  or  $err_{\ell^2}$ , but it is rather close to it, then the difference in the reconstructed images is almost negligible.

### 5.2. Non-inverse crime setting

In the inverse crime setting [16] the operator used in the reconstruction process is exactly the same of the one used for generating the synthetic data. Therefore, the tests we performed and showed in section 5.1 are compliant with the hypotheses of the theorems and must reflect their theoretical properties. However, in real world applications, the *exact* PSF of an acquisition instrument is not known (it does not necessarily exist) and therefore an *approximated* PSF is often used for the reconstruction process. In this case the forward model used to generate the data is not exactly the same used during the inversion process and this framework is called non-inverse crime setting. In order to study the behaviour of the stopping criteria presented in the previous section, in the non-inverse crime setting, inspired by the idea that a signal formation process is usually more complex than its mathematical formalization, first we simulate a more realistic image formation process by using an uneven PSF to generate the data and then we perform the inversion by using a smooth approximation of such a PSF. Therefore, we consider to generate the exact PSF of a given image formation process by following the procedure proposed in [4]: first we multiply by  $10^4$  the PSF used in the tests of section 5.1, then we add Poisson noise and finally we normalize the result. In this way we obtain an irregularly shaped PSF which we consider to be the *exact* PSF. Then, in the reconstruction process we make use of the smooth Gaussian shaped PSF described in section 5.1 intended to be a smooth approximation of the exact PSF. We report in figure 4 a comparison between the exact and the approximated PSF.

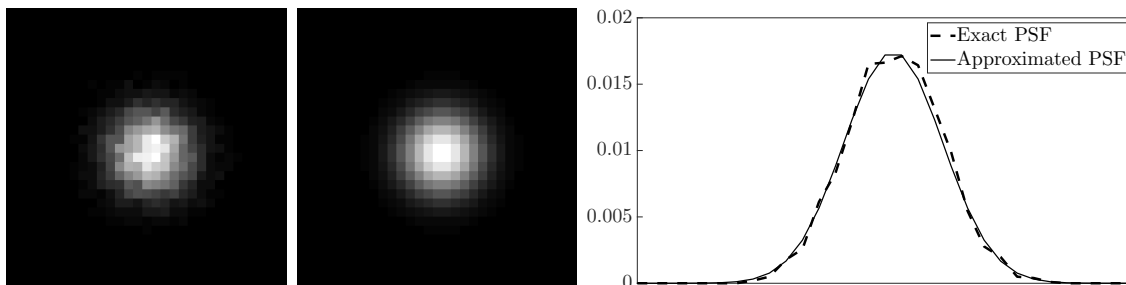


**Figure 4.** From left to right: the exact PSF, the approximated PSF and the profile of the exact (dashed line) and the approximated (solid line) PSF along an axis passing through the image center.

It is well known that, in practical applications, the discrepancy principle in the Gaussian framework requires a tuning parameter to work [20]. The main difficulty in real world problems is to determine a value for that parameters that makes the discrepancy principle sufficiently robust and reliable. We show now that, without a similar parameter, the discrepancy principle for Poisson data suffers from the same problem of the Gaussian case, i.e. sometimes it fails to work (as a stopping rule for the EM algorithm) in realistic simulation when the statistic of the data is high. Moreover, we show with some tests that the stopping rules based on the predictive risk seem to be more stable (at least in some cases and for some level of statistic). Finally, we give some

intuitive explanations for these behaviours (under appropriate hypothesis), without the presumption of being exhaustive in the treatment, but with the only aim to highlight the necessity of a deeper investigation concerning errors in the forward model.

We perform reconstructions from data generated by applying the irregularly shaped PSF to the images of nebula NGC7027 and of the Horse Head nebula. Again, we consider three levels of statistic: the total flux is equal to  $5 \times 10^8$ ,  $10^9$  and  $5 \times 10^9$  for the NGC7027 nebula and it is equal to  $1 \times 10^{10}$ ,  $2.5 \times 10^{10}$  and  $5 \times 10^{10}$  for the Horse Head nebula in the low, medium and high statistic case respectively. For both images, the same background of the tests of section 5.1 is added. This time we perform reconstructions for only one realization of Poisson noise in order to verify what can be the behaviour of the different stopping rules in a realistic application. We compute at every iteration the quantities described in section 5.1, i.e. the PE, the estimators of the risk (PAUKL, PUKLA and REKL), the reconstruction errors  $\text{err}_{\ell^2}$  and  $\text{err}_{\text{KL}}$ , the discrepancy  $d_{\text{KL}}$  and the PDP. We report in the left panel of figure 5 a plot of the discrepancy  $d_{\text{KL}}$  for the three different levels of statistic together with a horizontal line at  $M/2$  computed for the nebula NGC7027 image. In the right panel of figure 5 instead, we show the behaviour of the PE and of the proposed estimator in the medium statistic case for the nebula NGC7027. We also compare their optimal iterates with the ones of the reconstruction errors. Finally, in table 2 we report the number of iterations at which the quantities described above are minimized for the images of both nebula NGC7027 and Horse Head nebula in the three levels of statistic.

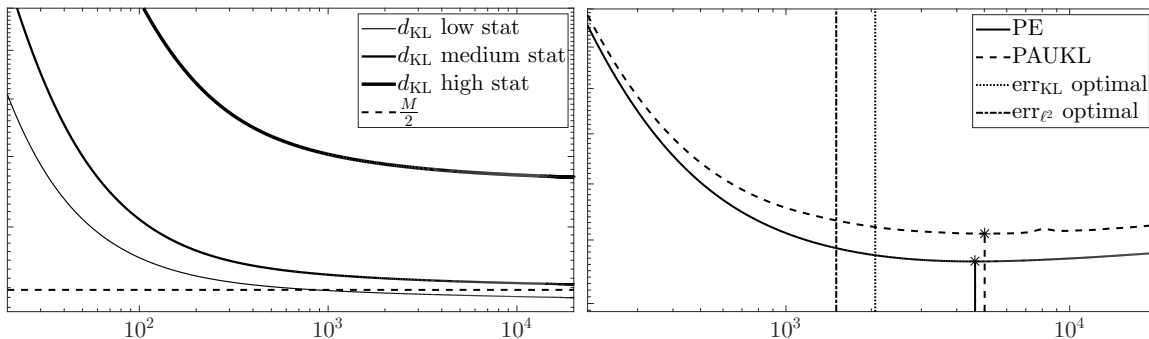


**Figure 5.** Left: discrepancy in KL divergence along the iterations for different levels of statistic for the nebula NGC7027. Solid lines represents the  $d_{\text{KL}}$  in the low, medium and high statistic case (low, medium and high thickness respectively) and dashed line is the asymptotic variance level. Right: PE (solid line) and PAUKL (dashed line) computed for the nebula NGC7027 in the medium statistic case. We indicate with a vertical line the iterate at which  $\text{err}_{\text{KL}}$  and  $\text{err}_{\ell^2}$  are minimized (dot-dashed line and dotted line respectively). In each figure the number of iterations is reported on the x-axis. Both figures are plotted in logarithmic scale on the x and on the y-axis.

We observe that the Poisson discrepancy principle is satisfied just in the low statistic case for both images (see table 2). An explanation for this behaviour can be found in figure 5 left panel. The line corresponding to the discrepancy gets more and more high with increasing statistic while the asymptotic variance does not depend on the statistic



Statistic	PE	PAUKL	PUKLA	REKL	PDP	$\text{err}_{\text{KL}}$	$\text{err}_{\ell^2}$
<b>NGC7027</b>							
Low	1606	1719	1537	1653	857	1224	832
Medium	4639	5014	6012	3985	*	2063	1503
High	*	*	*	*	*	3026	2869
<b>Horse Head</b>							
Low	1874	1749	1817	1718	689	1295	1457
Medium	5647	5530	6246	5072	*	2195	2476
High	*	*	*	*	*	3056	3468

**Table 2.** Comparison between the number of iterations that minimizes the PE, the estimators of the predictive risk (PAUKL, PUKLA and REKL), the PDP and the reconstruction errors ( $\text{err}_{\text{KL}}$  and  $\text{err}_{\ell^2}$ ). We indicate with an asterisk if after  $2 \times 10^4$  iterations the minimum has not been reached.

of the data. The error introduced by approximating an uneven PSF with an ideal one is reflected in an offset in the discrepancy that does not let it go below  $M/2$  (neither for  $k = +\infty$ ). In the next Lemma we show that such an offset depends on the specific data sample and on its geometric relation with respect to the image of the nonnegative orthant through the forward operator. Throughout this work we denoted by  $H$  the matrix corresponding to the ideal PSF. Here we denote by  $\hat{H}$  the matrix corresponding to the exact PSF. Given a matrix  $C \in \mathbb{R}^{M \times N}$  we also define the cone

$$\mathcal{R}_+(C) := \{Cx : x \in \mathbb{R}_+^N\} , \quad (42)$$

which contains all the possible values of a nonnegative vector through the matrix operator  $C$ . Hereafter, to simplify the computation and give a direct intuition of the next Lemma, we consider the EM algorithm with background  $b = 0$ . The function  $R_k$  defined in (12) is then positively homogeneous of degree 1, i.e.  $R_k(Ly) = LR_k(y)$  for all  $L > 0$  and for all  $y \in \mathbb{R}_+^M$  (see [2]).

**Lemma 5.1** *Let  $y$  be a realization of  $Y \sim \mathcal{P}(\hat{H}x)$  such that  $y \notin \mathcal{R}_+(H)$ . Then, if  $\|y\|$  is sufficiently large, for all  $k \in \mathbb{N}$*

$$D_{\text{KL}}(y, HR_k(y)) > \frac{M}{2} . \quad (43)$$

*Proof:* From the positive homogeneity of  $R_k$  it follows

$$D_{\text{KL}}(y, HR_k(y)) = \|y\| D_{\text{KL}}(\bar{y}, HR_k(\bar{y})) , \quad (44)$$

where  $\bar{y} := y/\|y\|$ . Now, thanks to the properties of the EM algorithm (see [19, 37]), for all  $k \in \mathbb{N}$  we have

$$D_{\text{KL}}(\bar{y}, HR_k(\bar{y})) \geq \lim_{k \rightarrow +\infty} D_{\text{KL}}(\bar{y}, HR_k(\bar{y})) = D_{\text{KL}}(\bar{y}, \lim_{k \rightarrow +\infty} HR_k(\bar{y})) . \quad (45)$$

As the sequence  $\{HR_k(\bar{y})\}_{k \in \mathbb{N}}$  converges to  $y^* \in \mathcal{R}_+(H)$  and as  $\bar{y} \notin \mathcal{R}_+(H)$ , then

$$D_{\text{KL}}(\bar{y}, HR_k(\bar{y})) \geq D_{\text{KL}}(\bar{y}, y^*) > 0. \quad (46)$$

Then, by taking

$$\|y\| \geq M/2(D_{\text{KL}}(\bar{y}, y^*))^{-1} \quad (47)$$

the thesis is straightforward.  $\square$

We point out that the conditions under which we prove Lemma 5.1 do not meet entirely the conditions under which we have developed the theory of this paper: this result is meant just to be a starting point for further investigations. In view of this, the thesis of Lemma 5.1 holds true even if  $y$  is a realization of  $Y \sim \mathcal{P}(Hx)$ , i.e. in the inverse crime case, as the crucial hypothesis is that  $y \notin \mathcal{R}_+(H)$ . However, for large scale problem the realization  $y$  is typically not too far from  $\mathcal{R}_+(H)$  in the sense that  $D_{\text{KL}}(\bar{y}, y^*)$  is small. In this scenario, the norm  $\|y\|$  must be so large to satisfy equation (47) that this case is really unlikely to happen in practice. Furthermore, an extremely large number of counts corresponds to a large signal-to-noise ratio and then regularization plays a minor role. What does really matter in this setting is the systematic error in the forward modelling which may increase  $D_{\text{KL}}(\bar{y}, y^*)$  to such an extent that the Poisson discrepancy principle does not work. An example of this is shown in the left panel of figure 5.

On the other hand, the stopping rule based on our estimator selects the iterate  $k$  that satisfies

$$D_{\text{KL}}(y, HR_k(y)) - D_{\text{KL}}(y, HR_{k+1}(y)) < (y\nabla) \cdot \log \frac{HR_{k+1}(y)}{HR_k(y)} \quad (48)$$

and therefore does not suffer from the presence of an offset in the case in which  $y \notin \mathcal{R}_+(H)$ ; this fact makes risk-based methods usually more robust with respect to the Poisson discrepancy principle. The stopping rule is always effective as long as the rate with which the KL divergence decreases along the iterations is definitely lower than the rate with which the term involving the trace increases. However, in the non-inverse crime setting there are problems due to the incorrect forward model used that make our stopping rule not work with high statistic level (see table 2). It is difficult to formalize the reasons of this misbehaviour as we did in Lemma 5.1 for the Poisson discrepancy principle. However, the crucial point is in the ill-posedness of the inverse problem since we notice that as long as the predictive risk estimator does not reach a minimum value along the iterations, also the PE, which is computed with the knowledge of  $\lambda$ , does not reach a minimum (see table 2, high statistic case).

## 6. Conclusions

As already remarked, in the case of the EM algorithm, the above mentioned predictive risk estimators do not differ each other, providing an alternative to the Poisson discrepancy principle, exactly as SURE does with respect to the Morozov's discrepancy principle. However, the proven theoretical results provide a more sound basis of the

proposed estimator and allow identifying the analogy between the Gaussian and the Poisson case. Besides proving a more general Stein's Lemma for Poisson data, we also introduced an estimator that is asymptotically unbiased, approximating the exact value of the predictive risk, unlike PUKLA or REKL that include an unknown constant offset as bias term, while preserving the same computational efficiency. Moreover, we give some simple conditions which has to be verified by a regularization method in order to make this estimator asymptotically unbiased. Therefore, this estimator can be efficiently used in selecting the regularization parameter of any algorithm that satisfies such conditions. The need of a suitable regularization is evident when the object to retrieve contains structures like edges or finer details. The analysis of other regularization methods may be the next direction of this work. Finally, as suggested by the numerical experiments reported in this paper, a theoretical investigation of the non-inverse crime case, also presented in this paper, is a crucial point for understanding the range of applicability of the proposed method.

## Acknowledgments

The authors thank the National Group of Scientific Computing (GNCS-INDAM) that supported this research.

## Appendix

In the following we will denote  $\pi_\lambda$  the probability mass function of an  $M$ -dimensional Poisson random variable with independent components and mean value  $\lambda \in \mathbb{R}_{++}^M$ , i.e.

$$\pi_\lambda(n) := \prod_{i=1}^M \frac{e^{-\lambda_i} \lambda_i^{n_i}}{n_i!} \quad \forall n \in \mathbb{N}^M. \quad (\text{A.1})$$

Moreover, if  $I \subseteq \{1, \dots, M\}$  is a subset of indices, we will pose

$$\|y\|_I := \sqrt{\sum_{i \in I} y_i^2} \quad (\text{A.2})$$

for all  $y \in \mathbb{R}^M$ . Finally, the inequalities between vectors and the integer part  $\lfloor \cdot \rfloor$  applied to vectors are meant component-wise.

The result proved in the next Lemma follows what done in [40].

**Lemma Appendix A.1** *There exist  $\eta > 0$  and  $0 < \theta < e$  such that, for all  $x > 0$ , we have*

$$g(x) := \frac{x^{\lfloor \frac{x}{2} \rfloor}}{\lfloor \frac{x}{2} \rfloor!} \leq \eta \theta^{\frac{x}{2}} e^{\frac{x}{2}} \quad (\text{A.3})$$

*Proof:* We consider three cases.

- 1) If  $0 < x \leq 2$ , then  $g(x) \leq 2$ .

2) If  $2 < x \leq 6$ , by using the Stirling lower bound of the factorial, we obtain

$$\left\lfloor \frac{x}{2} \right\rfloor! \geq \sqrt{2\pi} \left\lfloor \frac{x}{2} \right\rfloor^{\left\lfloor \frac{x}{2} \right\rfloor + \frac{1}{2}} e^{-\left\lfloor \frac{x}{2} \right\rfloor} \geq \sqrt{2\pi} \left\lfloor \frac{x}{2} \right\rfloor^{\left\lfloor \frac{x}{2} \right\rfloor} e^{-\frac{x}{2}}, \quad (\text{A.4})$$

therefore

$$g(x) \leq \frac{1}{\sqrt{2\pi}} e^{\frac{x}{2}} \left( \frac{x}{\left\lfloor \frac{x}{2} \right\rfloor} \right)^{\left\lfloor \frac{x}{2} \right\rfloor}. \quad (\text{A.5})$$

Moreover, as

$$\left( \frac{x}{\left\lfloor \frac{x}{2} \right\rfloor} \right)^{\left\lfloor \frac{x}{2} \right\rfloor} = e^{\left\lfloor \frac{x}{2} \right\rfloor \log x} e^{-\left\lfloor \frac{x}{2} \right\rfloor \log \left\lfloor \frac{x}{2} \right\rfloor} \leq e^{3 \log 6} = 216, \quad (\text{A.6})$$

we obtain

$$g(x) \leq \frac{216}{\sqrt{2\pi}} e^{\frac{x}{2}}. \quad (\text{A.7})$$

3) If  $x > 6$ , using again (A.5) and observing that

$$2 \leq \frac{x}{\left\lfloor \frac{x}{2} \right\rfloor} \leq \frac{8}{3} \simeq 2.67 < e \quad (\text{A.8})$$

leads to

$$g(x) \leq \frac{1}{\sqrt{2\pi}} e^{\frac{x}{2}} \left( \frac{8}{3} \right)^{\frac{x}{2}}. \quad (\text{A.9})$$

We conclude by posing  $\eta = \frac{216}{\sqrt{2\pi}}$  and  $\theta = \frac{8}{3}$ .  $\square$

**Lemma Appendix A.2** *There exist  $c > 0$  such that*

$$\sum_{n \leq \left\lfloor \frac{\lambda}{2} \right\rfloor} \pi_\lambda(n) = O(\|\lambda\|^M e^{-c\|\lambda\|}) \quad (\text{A.10})$$

as  $\|\lambda\| \rightarrow +\infty$  in  $\mathbb{R}_{++}^M$ .

*Proof:* By definition we have

$$\sum_{n \leq \left\lfloor \frac{\lambda}{2} \right\rfloor} \pi_\lambda(n) = \prod_{i=1}^M \sum_{n_i=1}^{\left\lfloor \frac{\lambda_i}{2} \right\rfloor} \frac{e^{-\lambda_i} \lambda_i^{n_i}}{n_i!}. \quad (\text{A.11})$$

Following what done in [40], by using the fact that  $\lambda_i^r/r! < \lambda_i^s/s!$  when  $r < s \leq \left\lfloor \frac{\lambda_i}{2} \right\rfloor$ , we obtain

$$\sum_{n_i=0}^{\left\lfloor \frac{\lambda_i}{2} \right\rfloor} \frac{e^{-\lambda_i} \lambda_i^{n_i}}{n_i!} \leq \left( \left\lfloor \frac{\lambda_i}{2} \right\rfloor + 1 \right) e^{-\lambda_i} \frac{\lambda_i^{\left\lfloor \frac{\lambda_i}{2} \right\rfloor}}{\left\lfloor \frac{\lambda_i}{2} \right\rfloor!}. \quad (\text{A.12})$$

Now, thanks to Lemma Appendix A.1, there exist  $\eta > 0$  and  $0 < \theta < e$  such that

$$\frac{\lambda_i^{\left\lfloor \frac{\lambda_i}{2} \right\rfloor}}{\left\lfloor \frac{\lambda_i}{2} \right\rfloor!} \leq \eta \theta^{\frac{\lambda_i}{2}} e^{\frac{\lambda_i}{2}}, \quad (\text{A.13})$$

therefore

$$\sum_{n_i=0}^{\lfloor \frac{\lambda_i}{2} \rfloor} \frac{e^{-\lambda_i} \lambda_i^{n_i}}{n_i!} \leq \eta \left( \left\lfloor \frac{\lambda_i}{2} \right\rfloor + 1 \right) e^{-\lambda_i} \theta^{\frac{\lambda_i}{2}} e^{\frac{\lambda_i}{2}} \leq \eta \left( \frac{\lambda_i}{2} + 1 \right) \left( \frac{e}{\theta} \right)^{-\frac{\lambda_i}{2}}. \quad (\text{A.14})$$

If we denote  $a := e/\theta > 1$  and if we use the fact that  $\lambda_i \leq \|\lambda\|$  in  $\mathbb{R}_{++}^M$ , we have

$$\prod_{i=1}^M \sum_{n_i=1}^{\lfloor \frac{\lambda_i}{2} \rfloor} \frac{e^{-\lambda_i} \lambda_i^{n_i}}{n_i!} \leq \eta^M \left( \frac{\|\lambda\|}{2} + 1 \right)^M a^{-\frac{\|\lambda\|_1}{2}}. \quad (\text{A.15})$$

Hence, as  $\|\lambda\|_1 \geq \|\lambda\|$ , we obtain

$$\sum_{n \leq \lfloor \frac{\lambda}{2} \rfloor} \pi_\lambda(n) \leq \eta^M \left( \frac{\|\lambda\|}{2} + 1 \right)^M a^{-\frac{\|\lambda\|}{2}} = \eta^M \left( \frac{\|\lambda\|}{2} + 1 \right)^M e^{-\frac{\|\lambda\|}{2} \log a}. \quad (\text{A.16})$$

The thesis is straightforward if we pose  $c := (\log a)/2 > 0$ .  $\square$

**Lemma Appendix A.3** *Let  $I \subseteq \{1, \dots, M\}$  be a nonempty subset of indices and let  $\mathcal{C} \subset \mathbb{R}_{++}^M$  be a closed convex cone. Then, there exist  $c_1, c_2 > 0$  such that  $c_1 \|y\| \leq \|y\|_I \leq c_2 \|y\|$  for all  $y \in \mathcal{C}$ .*

*Proof:* We can trivially take  $c_2 = 1$  as  $\|y\|_I \leq \|y\|$ . Now, let us pose

$$g(y) := \frac{\|y\|_I}{\|y\|}. \quad (\text{A.17})$$

We want to prove that there exists  $c_1 > 0$  such that  $g(y) \geq c_1$  for all  $y \in \mathcal{C} \setminus \{0\}$ . We observe that  $g$  is continuous on  $\mathbb{R}_+^M \setminus \{0\}$  and that it is positively homogeneous of degree 0, i.e.  $g(Ly) = g(y)$  for all  $y \in \mathbb{R}_+^M \setminus \{0\}$  and for all  $L > 0$ . We point out that  $\mathcal{C} \cap \mathbb{S}^{M-1}$  (where  $\mathbb{S}^{M-1}$  denotes the surface of the unit sphere in  $\mathbb{R}^M$ ) is a compact set, therefore, for Weierstrass Theorem,  $g$  attains a minimum value  $c_1$  on it. Moreover, as  $\mathcal{C} \cap \mathbb{S}^{M-1}$  it holds  $c_1 > 0$ . If we consider  $y \in \mathcal{C} \setminus \{0\}$ , then, thanks to the positive homogeneity of degree 0 of  $g$  and thanks to the fact that  $y/\|y\| \in \mathcal{C} \cap \mathbb{S}^{M-1}$ , we have

$$g(y) = g\left(\|y\| \frac{y}{\|y\|}\right) = g\left(\frac{y}{\|y\|}\right) \geq c_1. \quad (\text{A.18})$$

$\square$

*Proof of Lemma 3.1:* By adding and subtracting  $\lambda_i \partial_i f(\lambda)$ , we have

$$\begin{aligned} \mathbb{E}((Y_i - \lambda_i) f(Y) - Y_i \partial_i f(Y)) &= \mathbb{E}((Y_i - \lambda_i) f(Y) - \lambda_i \partial_i f(\lambda)) + \\ &\quad \mathbb{E}(\lambda_i \partial_i f(\lambda) - Y_i \partial_i f(Y)). \end{aligned} \quad (\text{A.19})$$

Hence, we prove

$$\mathbb{E}((Y_i - \lambda_i) f(Y) - \lambda_i \partial_i f(\lambda)) = O(\|\lambda\|^{-1/2}) \quad (\text{A.20})$$

and

$$\mathbb{E}(\lambda_i \partial_i f(\lambda) - Y_i \partial_i f(Y)) = O(\|\lambda\|^{-1/2}) \quad (\text{A.21})$$

as  $\|\lambda\| \rightarrow +\infty$  in  $\mathcal{C}$  (actually, we will give only the proof of (A.20) as the one of (A.21) is analogous). If we apply Taylor formula with Lagrange remainder to  $f$  we have

$$f(Y) = f(\lambda) + \sum_{j=1}^M \partial_j f(\lambda)(Y_j - \lambda_j) + \frac{1}{2} \sum_{k,l=1}^M \partial_k \partial_l f(\xi_{\lambda,Y})(Y_k - \lambda_k)(Y_l - \lambda_l) , \quad (\text{A.22})$$

where  $\xi_{\lambda,Y} = \lambda + t(Y - \lambda)$  for some  $t \in (0, 1)$ . Therefore,

$$\begin{aligned} & \mathbb{E}((Y_i - \lambda_i) f(Y) - \lambda_i \partial_i f(\lambda)) = \\ & f(\lambda) \mathbb{E}(Y_i - \lambda_i) + \left[ \sum_{j=1}^M \partial_j f(\lambda) \mathbb{E}((Y_i - \lambda_i)(Y_j - \lambda_j)) - \lambda_i \partial_i f(\lambda) \right] + \\ & \frac{1}{2} \sum_{k,l=1}^M \mathbb{E}(\partial_k \partial_l f(\xi_{\lambda,Y})(Y_i - \lambda_i)(Y_k - \lambda_k)(Y_l - \lambda_l)) . \end{aligned} \quad (\text{A.23})$$

Now, as  $\mathbb{E}(Y_i - \lambda_i) = 0$  and  $\mathbb{E}((Y_i - \lambda_i)(Y_j - \lambda_j)) = \delta_{ij} \lambda_i$ , where  $\delta_{ij}$  denotes the Kronecker symbol, we obtain

$$\begin{aligned} & \mathbb{E}((Y_i - \lambda_i) f(Y) - \lambda_i \partial_i f(\lambda)) = \\ & \frac{1}{2} \sum_{k,l=1}^M \mathbb{E}(\partial_k \partial_l f(\xi_{\lambda,Y})(Y_i - \lambda_i)(Y_k - \lambda_k)(Y_l - \lambda_l)) . \end{aligned} \quad (\text{A.24})$$

Let us fix  $k, l \in \{1, \dots, M\}$ . We want to prove that

$$\mathbb{E}(\partial_k \partial_l f(\xi_{\lambda,Y})(Y_i - \lambda_i)(Y_k - \lambda_k)(Y_l - \lambda_l))^2 = O(\|\lambda\|^{-1}) \quad (\text{A.25})$$

as  $\|\lambda\| \rightarrow +\infty$  in  $\mathcal{C}$ . By applying Jensen's inequality and hypothesis (iv) we obtain

$$\begin{aligned} & (\mathbb{E}(\partial_k \partial_l f(\xi_{\lambda,Y})(Y_i - \lambda_i)(Y_k - \lambda_k)(Y_l - \lambda_l)))^2 \leq \\ & \mathbb{E}((\partial_k \partial_l f(\xi_{\lambda,Y}))^2 (Y_i - \lambda_i)^2 (Y_k - \lambda_k)^2 (Y_l - \lambda_l)^2) \leq \\ & \mathbb{E}\left(\frac{c_{k,l}^2}{(\|\xi_{\lambda,Y}\|^2 + \varepsilon_{k,l})^2} (Y_i - \lambda_i)^2 (Y_k - \lambda_k)^2 (Y_l - \lambda_l)^2\right) = \\ & c_{k,l}^2 \sum_{n \in \mathbb{N}^M} \frac{1}{(\|\xi_{\lambda,n}\|^2 + \varepsilon_{k,l})^2} (n_i - \lambda_i)^2 (n_k - \lambda_k)^2 (n_l - \lambda_l)^2 \pi_\lambda(n) . \end{aligned} \quad (\text{A.26})$$

We point out that  $\mathbb{N}^M$  can be written as a finite union of disjoint sets as follows

$$\mathbb{N}^M = \bigcup_{p=0}^{2^M-1} \mathcal{A}_\lambda^p , \quad (\text{A.27})$$

where, if we denote by  $p_i$  the  $i$ -th bit in the binary representation of  $p$ , then

$$\mathcal{A}_\lambda^p := \left\{ n \in \mathbb{N}^M : (-1)^{p_i} \left( n_i - \left\lfloor \frac{\lambda_i}{2} \right\rfloor - p_i \right) \leq 0 \quad \forall i \in \{1, \dots, M\} \right\} ; \quad (\text{A.28})$$

moreover, we pose

$$I_\leq^p := \{i \in \{1, \dots, M\} : p_i = 0\} , \quad I_\geq^p := \{i \in \{1, \dots, M\} : p_i = 1\} . \quad (\text{A.29})$$

Now, it is easy to verify that

$$\|\xi_{\lambda,n}\| \geq \frac{\|\lambda\|_{I_\leq^p}}{2} , \quad (\text{A.30})$$

therefore

$$\sum_{n \in \mathbb{N}^M} \frac{1}{(\|\xi_{\lambda,n}\|^2 + \varepsilon_{k,l})^2} (n_i - \lambda_i)^2 (n_k - \lambda_k)^2 (n_l - \lambda_l)^2 \pi_{\lambda}(n) \leq \sum_{p=0}^{2^M-1} \varphi_{p,k,l}(\lambda) , \quad (\text{A.31})$$

with

$$\varphi_{p,k,l}(\lambda) := \frac{16}{(\|\lambda\|_{I_{\geq}^p}^2 + 4\varepsilon_{k,l})^2} \sum_{n \in \mathcal{A}_{\lambda}^p} (n_i - \lambda_i)^2 (n_k - \lambda_k)^2 (n_l - \lambda_l)^2 \pi_{\lambda}(n) . \quad (\text{A.32})$$

Let us focus on

$$\sum_{n \in \mathcal{A}_{\lambda}^p} (n_i - \lambda_i)^2 (n_k - \lambda_k)^2 (n_l - \lambda_l)^2 \pi_{\lambda}(n) . \quad (\text{A.33})$$

Denoted  $\overline{M}$  the cardinality of  $I_{\leq}^p$ , with  $0 \leq \overline{M} \leq M$ , we distinguish four cases.

1)  $i, k, l \in I_{\leq}^p$ . Then,

$$\begin{aligned} & \sum_{n \in \mathcal{A}_{\lambda}^p} (n_i - \lambda_i)^2 (n_k - \lambda_k)^2 (n_l - \lambda_l)^2 \pi_{\lambda}(n) \leq \\ & \left( \prod_{q \in I_{\leq}^p} \sum_{n_q=0}^{\lfloor \frac{\lambda_q}{2} \rfloor} \frac{e^{-\lambda_q} \lambda_q^{n_q}}{n_q!} \right) \left( \prod_{r \in I_{\geq}^p} \sum_{n_r=0}^{+\infty} (n_i - \lambda_i)^2 (n_k - \lambda_k)^2 (n_l - \lambda_l)^2 \frac{e^{-\lambda_r} \lambda_r^{n_r}}{n_r!} \right) . \end{aligned} \quad (\text{A.34})$$

The first term can be bounded by using Lemma Appendix A.2 and Lemma Appendix A.3, obtaining

$$\prod_{q \in I_{\leq}^p} \sum_{n_q=0}^{\lfloor \frac{\lambda_q}{2} \rfloor} \frac{e^{-\lambda_q} \lambda_q^{n_q}}{n_q!} = O\left(\|\lambda\|_{I_{\leq}^p}^{\overline{M}} e^{-c\|\lambda\|_{I_{\leq}^p}}\right) \quad (\text{A.35})$$

as  $\|\lambda\| \rightarrow +\infty$  in  $\mathcal{C}$ . For the second term we consider instead the moments about the mean of a Poisson distribution (see [24] pag. 162) and Lemma Appendix A.3 to have

$$\prod_{r \in I_{\geq}^p} \sum_{n_r=0}^{+\infty} (n_i - \lambda_i)^2 (n_k - \lambda_k)^2 (n_l - \lambda_l)^2 \frac{e^{-\lambda_r} \lambda_r^{n_r}}{n_r!} = O\left(\|\lambda\|_{I_{\geq}^p}^3\right) \quad (\text{A.36})$$

as  $\|\lambda\| \rightarrow +\infty$  in  $\mathcal{C}$ .

2) Only two of  $i, k, l$  belong to  $I_{\geq}^p$  (in order to fix the ideas we assume  $i, k \in I_{\geq}^p$  and  $l \in I_{\leq}^p$ ). Then,

$$\begin{aligned} & \sum_{n \in \mathcal{A}_{\lambda}^p} (n_i - \lambda_i)^2 (n_k - \lambda_k)^2 (n_l - \lambda_l)^2 \pi_{\lambda}(n) \leq \\ & \left( \prod_{q \in I_{\leq}^p} \sum_{n_q=0}^{\lfloor \frac{\lambda_q}{2} \rfloor} (n_l - \lambda_l)^2 \frac{e^{-\lambda_q} \lambda_q^{n_q}}{n_q!} \right) \left( \prod_{r \in I_{\geq}^p} \sum_{n_r=0}^{+\infty} (n_i - \lambda_i)^2 (n_k - \lambda_k)^2 \frac{e^{-\lambda_r} \lambda_r^{n_r}}{n_r!} \right) . \end{aligned} \quad (\text{A.37})$$

We observe that  $(n_l - \lambda_l)^2 \leq \lambda_l^2 \leq \|\lambda\|_{I_{\leq}^p}^2$ , therefore, thanks to Lemma Appendix A.2 and Lemma Appendix A.3, we obtain

$$\prod_{q \in I_{\leq}^p} \sum_{n_q=0}^{\lfloor \frac{\lambda_q}{2} \rfloor} (n_l - \lambda_l)^2 \frac{e^{-\lambda_q} \lambda_q^{n_q}}{n_q!} = O\left(\|\lambda\|_{I_{\leq}^p}^{\overline{M}+2} e^{-c\|\lambda\|_{I_{\leq}^p}}\right) \quad (\text{A.38})$$

as  $\|\lambda\| \rightarrow +\infty$  in  $\mathcal{C}$ . Again, if we consider the moments about the mean of a Poisson distribution and Lemma Appendix A.3, we have

$$\prod_{r \in I_{\geq}^p} \sum_{n_r=0}^{+\infty} (n_i - \lambda_i)^2 (n_k - \lambda_k)^2 \frac{e^{-\lambda_r} \lambda_r^{n_r}}{n_r!} = O\left(\|\lambda\|_{I_{\geq}^p}^2\right) \quad (\text{A.39})$$

as  $\|\lambda\| \rightarrow +\infty$  in  $\mathcal{C}$ .

- 3) Only one of  $i, k, l$  belongs to  $I_{\geq}^p$  (in order to fix the ideas we assume  $i \in I_{\geq}^p$  and  $k, l \in I_{\leq}^p$ ). Then we have

$$\begin{aligned} & \sum_{n \in \mathcal{A}_{\lambda}^p} (n_i - \lambda_i)^2 (n_k - \lambda_k)^2 (n_l - \lambda_l)^2 \pi_{\lambda}(n) \leq \\ & \left( \prod_{q \in I_{\leq}^p} \sum_{n_q=0}^{\lfloor \frac{\lambda_q}{2} \rfloor} (n_k - \lambda_k)^2 (n_l - \lambda_l)^2 \frac{e^{-\lambda_q} \lambda_q^{n_q}}{n_q!} \right) \left( \prod_{r \in I_{\geq}^p} \sum_{n_r=0}^{+\infty} (n_i - \lambda_i)^2 \frac{e^{-\lambda_r} \lambda_r^{n_r}}{n_r!} \right) = \\ & \left( \prod_{q \in I_{\leq}^p} \sum_{n_q=0}^{\lfloor \frac{\lambda_q}{2} \rfloor} (n_k - \lambda_k)^2 (n_l - \lambda_l)^2 \frac{e^{-\lambda_q} \lambda_q^{n_q}}{n_q!} \right) \left( \sum_{n_i=0}^{+\infty} (n_i - \lambda_i)^2 \frac{e^{-\lambda_i} \lambda_i^{n_i}}{n_i!} \right) = \\ & \left( \prod_{q \in I_{\leq}^p} \sum_{n_q=0}^{\lfloor \frac{\lambda_q}{2} \rfloor} (n_k - \lambda_k)^2 (n_l - \lambda_l)^2 \frac{e^{-\lambda_q} \lambda_q^{n_q}}{n_q!} \right) \lambda_i. \end{aligned} \quad (\text{A.40})$$

We observe that  $(n_k - \lambda_k)^2 (n_l - \lambda_l)^2 \leq \lambda_k^2 \lambda_l^2 \leq \|\lambda\|_{I_{\leq}^p}^4$ . Thanks to Lemma Appendix A.2 and Lemma Appendix A.3 we obtain

$$\prod_{q \in I_{\leq}^p} \sum_{n_q=0}^{\lfloor \frac{\lambda_q}{2} \rfloor} (n_k - \lambda_k)^2 (n_l - \lambda_l)^2 \frac{e^{-\lambda_q} \lambda_q^{n_q}}{n_q!} = O\left(\|\lambda\|_{I_{\leq}^p}^{\overline{M}+4} e^{-c\|\lambda\|_{I_{\leq}^p}}\right), \quad (\text{A.41})$$

while trivially  $\lambda_i = O(\|\lambda\|_{I_{\geq}^p})$  as  $\|\lambda\| \rightarrow +\infty$  in  $\mathcal{C}$ .

- 4)  $i, k, l \in I_{\leq}^p$ . Then we have

$$\begin{aligned} & \sum_{n \in \mathcal{A}_{\lambda}^p} (n_i - \lambda_i)^2 (n_k - \lambda_k)^2 (n_l - \lambda_l)^2 \pi_{\lambda}(n) \leq \\ & \left( \prod_{q \in I_{\leq}^p} \sum_{n_q=0}^{\lfloor \frac{\lambda_q}{2} \rfloor} (n_i - \lambda_i)^2 (n_k - \lambda_k)^2 (n_l - \lambda_l)^2 \frac{e^{-\lambda_q} \lambda_q^{n_q}}{n_q!} \right). \end{aligned} \quad (\text{A.42})$$



Now, as  $(n_i - \lambda_i)^2 (n_k - \lambda_k)^2 (n_l - \lambda_l)^2 \leq \lambda_i^2 \lambda_k^2 \lambda_l^2 \leq \|\lambda\|_{I_{\leq}^p}^6$ , if we apply Lemma Appendix A.2 and Lemma Appendix A.3 we obtain

$$\sum_{q \in I_{\leq}^p, n_q=0}^{\lfloor \frac{\lambda_q}{2} \rfloor} (n_i - \lambda_i)^2 (n_k - \lambda_k)^2 (n_l - \lambda_l)^2 \frac{e^{-\lambda_q} \lambda_q^{n_q}}{n_q!} = O\left(\|\lambda\|_{I_{\leq}^p}^{\overline{M}+6} e^{-c_4 \|\lambda\|_{I_{\leq}^p}}\right) \quad (\text{A.43})$$

as  $\|\lambda\| \rightarrow +\infty$  in  $\mathcal{C}$ .

If we take into account all these facts we have

$$\varphi_{p,k,l}(\lambda) = O\left(\left(\|\lambda\|_{I_{\leq}^p}^{\overline{M}+6} e^{-c \|\lambda\|_{I_{\leq}^p}}\right) \frac{\|\lambda\|_{I_{\leq}^p}^3}{\left(\|\lambda\|_{I_{\leq}^p}^2 + 4\varepsilon_{k,l}\right)^2}\right) \quad (\text{A.44})$$

as  $\|\lambda\| \rightarrow +\infty$  in  $\mathcal{C}$ . If  $p < 2^M - 1$ , then there exist at least one bit equal to 0 in the binary decomposition of  $p$  and therefore  $I_{\leq}^p$  is not empty. If we apply Lemma Appendix A.3, we have that there exist  $c' > 0$  and a rational function  $g_p$  such that

$$\varphi_{p,k,l}(\lambda) = O\left(g_p(\|\lambda\|) e^{-c' \|\lambda\|}\right) \quad (\text{A.45})$$

as  $\|\lambda\| \rightarrow +\infty$  in  $\mathcal{C}$ , hence  $\varphi_{p,k,l}$  tends to zero exponentially fast. If  $p = 2^M - 1$ , then  $I_{\leq}^p = \emptyset$  and thanks to Lemma Appendix A.3

$$\varphi_{p,k,l}(\lambda) = O\left(\|\lambda\|^{-1}\right) \quad (\text{A.46})$$

as  $\|\lambda\| \rightarrow +\infty$  in  $\mathcal{C}$ . This proves (A.25) and therefore (A.20).  $\square$

*Proof of Theorem 3.1:* From some simple computations we obtain

$$\begin{aligned} \mathbb{E}(D_{\text{KL}}(\lambda, \hat{\lambda}(Y))) &= \\ \mathbb{E}(D_{\text{KL}}(Y, \hat{\lambda}(Y))) + \mathbb{E}\left(\sum_{i=1}^M (Y_i - \lambda_i) \log \hat{\lambda}(Y)\right) - \mathbb{E}\left(\sum_{i=1}^M Y_i \log \frac{Y_i}{\lambda_i}\right). \end{aligned} \quad (\text{A.47})$$

We point out that, thanks to Lemma Appendix A.3, if  $\|\lambda\| \rightarrow +\infty$  in the cone  $\mathcal{C}$ , then  $\lambda_i \rightarrow +\infty$  for all  $i \in \{1, \dots, M\}$ . Therefore, we can apply the result proved in [40] and Lemma Appendix A.3 to obtain

$$\mathbb{E}\left(\sum_{i=1}^M Y_i \log \frac{Y_i}{\lambda_i}\right) = \frac{M}{2} + O\left(\|\lambda\|^{-1}\right) \quad (\text{A.48})$$

as  $\|\lambda\| \rightarrow +\infty$  in  $\mathcal{C}$ . Finally, as a consequence of Lemma 3.1, we have

$$\mathbb{E}\left(\sum_{i=1}^M (Y_i - \lambda_i) \log \hat{\lambda}(Y)\right) = \mathbb{E}\left((Y \nabla) \cdot \log \hat{\lambda}(Y)\right) + O\left(\|\lambda\|^{-1/2}\right) \quad (\text{A.49})$$

as  $\|\lambda\| \rightarrow +\infty$  in  $\mathcal{C}$ .  $\square$

*Proof of Proposition 4.1:* We prove the thesis by induction. The case  $k = 1$  is trivial with  $d = 0$ , as for all  $j \in \{1, \dots, N\}$  we have

$$(R_1(y))_j = \sum_{i=1}^M \xi_{ji} y_i \quad (\text{A.50})$$

with

$$\xi_{ji} := \frac{(x_0)_j H_{ij}}{(H^T \mathbf{1})_j ((H x_0)_i + b)} > 0. \quad (\text{A.51})$$

Let us now assume

$$(R_k(y))_l = \frac{p_{k,l}^{(d+1)}(y) + \dots + p_{k,l}^{(0)}}{q_{k,l}^{(d)}(y) + \dots + q_{k,l}^{(0)}} \quad (\text{A.52})$$

satisfying (i) and (ii) for all  $l \in \{1, \dots, N\}$ . Then, for all  $i \in \{1, \dots, M\}$  we can write

$$(HR_k(y))_i + b = \frac{a_{k,i}^{(Nd+1)}(y) + \dots + a_{k,i}^{(0)}}{c_k^{(Nd)}(y) + \dots + c_k^{(0)}}, \quad (\text{A.53})$$

where the summands in the numerator and in the denominator of the right-hand side are homogeneous polynomials with nonnegative coefficients. In particular, as

$$a_{k,i}^{(Nd+1)}(y) := \sum_{l=1}^N H_{il} p_{k,l}^{(d+1)}(y) \left( \prod_{\substack{s=1 \\ s \neq l}}^N q_{k,s}^{(d)}(y) \right), \quad (\text{A.54})$$

$$c_k^{(Nd)}(y) := \prod_{t=1}^N q_{k,t}^{(d)}(y), \quad (\text{A.55})$$

and

$$a_{k,i}^{(0)} := \sum_{l=1}^N H_{il} p_{k,l}^{(0)} \left( \prod_{\substack{s=1 \\ s \neq l}}^N q_{k,s}^{(0)} \right) + b \left( \prod_{t=1}^N q_{k,t}^{(0)} \right), \quad (\text{A.56})$$

we point out that both  $a_{k,i}^{(Nd+1)}$  and  $c_k^{(Nd)}$  are complete and that  $a_{k,i}^{(0)} > 0$ . Hence, with some simple calculations, one can prove that for all  $j \in \{1, \dots, N\}$  it holds

$$\left( \frac{1}{H^T \mathbf{1}} H^T \left( \frac{y}{HR_k(y) + b} \right) \right)_j = \frac{\tilde{p}_{k,j}^{(M(Nd+1))}(y) + \dots + \tilde{p}_{k,j}^{(0)}}{\tilde{q}_k^{(M(Nd+1))}(y) + \dots + \tilde{q}_k^{(0)}}, \quad (\text{A.57})$$

where the numerator and the denominator of the right-hand side consist of sums of homogeneous polynomials with nonnegative coefficients; moreover, we can observe that

$$\tilde{p}_{k,j}^{(M(Nd+1))}(y) := \frac{c_k^{(Nd)}(y)}{(H^T \mathbf{1})_j} \left( \sum_{i=1}^M H_{ij} y_i \left( \prod_{\substack{r=1 \\ r \neq i}}^M a_{k,r}^{(Nd+1)}(y) \right) \right) \quad (\text{A.58})$$

and

$$\tilde{q}_k^{(M(Nd+1))}(y) := \prod_{i=1}^M a_{k,i}^{(Nd+1)}(y) \quad (\text{A.59})$$

are complete and that

$$\tilde{q}_k^{(0)} := \prod_{i=1}^M a_{k,i}^{(0)} > 0. \quad (\text{A.60})$$

If we use (A.52) and (A.57) we obtain

$$(R_{k+1}(y))_j = \frac{p_{k,j}^{(d+1)}(y) + \dots + p_{k,j}^{(0)}}{q_{k,j}^{(d)}(y) + \dots + q_{k,j}^{(0)}} \cdot \frac{\tilde{p}_{k,j}^{(M(Nd+1))}(y) + \dots + \tilde{p}_{k,j}^{(0)}}{\tilde{q}_k^{(M(Nd+1))}(y) + \dots + \tilde{q}_k^{(0)}}. \quad (\text{A.61})$$

Therefore we can write

$$(R_{k+1}(y))_j = \frac{p_{k+1,j}^{(\bar{d}+1)}(y) + \dots + p_{k+1,j}^{(0)}}{q_{k+1,j}^{(\bar{d})}(y) + \dots + q_{k+1,j}^{(0)}}, \quad (\text{A.62})$$

where  $\bar{d} = (MN + 1)d + M$  and

- (i)  $p_{k+1,j}^{(n)}, q_{k+1,j}^{(m)}$  are homogeneous polynomials with nonnegative coefficients for all  $n \in \{1, \dots, \bar{d} + 1\}$  and for all  $m \in \{1, \dots, \bar{d}\}$ ;
- (ii)  $p_{k+1,j}^{(\bar{d}+1)}, q_{k+1,j}^{(\bar{d})}$  are complete and  $q_{k+1,j}^{(0)} > 0$  as

$$p_{k+1,j}^{(\bar{d}+1)}(y) := p_{k,j}^{(d+1)}(y) \cdot \tilde{p}_{k,j}^{(M(Nd+1))}(y), \quad (\text{A.63})$$

$$q_{k+1,j}^{(\bar{d})}(y) := q_{k,j}^{(d)}(y) \cdot \tilde{q}_k^{(M(Nd+1))}(y), \quad (\text{A.64})$$

and

$$q_{k+1,j}^{(0)} := q_{k,j}^{(0)} \cdot \tilde{q}_k^{(0)}. \quad (\text{A.65})$$

□

*Proof of Proposition 4.2:* It follows from Proposition 4.1 that  $(\hat{\lambda}_k)_i \in C^\infty(\mathbb{R}_+^M)$ . As  $(\hat{\lambda}_k)_i$  is strictly positive on  $\mathbb{R}_+^M$ , then  $(\log \hat{\lambda}_k)_i$  is well defined and belongs to  $C^\infty(\mathbb{R}_+^M)$ , hence (i). Let us prove (ii). As a consequence of Proposition 4.1, one can easily prove that, for all  $j \in \{1, \dots, M\}$

$$\partial_j(\log \hat{\lambda}_k)_i(y) = \frac{p^{(d)}(y) + \dots + p^{(0)}}{q^{(d+1)}(y) + \dots + q^{(0)}} \quad (\text{A.66})$$

with  $d \in \mathbb{N}$  and  $p^{(n)}, q^{(m)}$  homogeneous polynomials of degree  $n$  and  $m$  respectively for all  $n \in \{1, \dots, d\}$  and for all  $m \in \{1, \dots, d + 1\}$ . Moreover, the polynomials in the denominator have nonnegative coefficients,  $q^{(d+1)}$  is complete and  $q^{(0)} > 0$ . Since  $y_i \leq \|y\|$  for all  $y \in \mathbb{R}_+^M$ , there exist  $\tilde{p}_0, \dots, \tilde{p}_d > 0$  such that

$$|p^{(d)}(y) + \dots + p^{(0)}| \leq \tilde{p}_d \|y\|^d + \dots + \tilde{p}_0. \quad (\text{A.67})$$

Moreover, for Weierstrass Theorem there exists  $\tilde{q}_{d+1} \geq 0$  such that

$$\left| q^{(d+1)}\left(\frac{y}{\|y\|}\right) \right| \geq \tilde{q}_{d+1} \quad (\text{A.68})$$

for all  $y \in \mathbb{R}_+^M \setminus \{0\}$ . The completeness of  $q^{(d+1)}$  allows us to conclude that  $\tilde{q}_{d+1} > 0$ . If  $y \in \mathbb{R}_+^M \setminus \{0\}$ , then

$$|q^{(d+1)}(y)| = \|y\|^{d+1} \left| q^{(d+1)} \left( \frac{y}{\|y\|} \right) \right| \geq \tilde{q}_{d+1} \|y\|^{d+1} \quad (\text{A.69})$$

(actually, the inequality  $|q^{(d+1)}(y)| \geq \tilde{q}_{d+1} \|y\|^{d+1}$  holds true for all  $y \in \mathbb{R}_+^M$ ). Therefore,

$$|q^{(d+1)}(y) + \dots + q^{(0)}| \geq \tilde{q}_{d+1} \|y\|^{d+1} + q^{(0)}. \quad (\text{A.70})$$

By taking into account (A.67) and (A.70) we obtain

$$\begin{aligned} |\partial_j(\log \hat{\lambda}_k)_i(y)| &\leq \frac{\tilde{p}_d \|y\|^d + \dots + \tilde{p}_0}{\tilde{q}_{d+1} \|y\|^{d+1} + q^{(0)}} = \\ &\tilde{p}_d \frac{\|y\|^d}{\tilde{q}_{d+1} \|y\|^{d+1} + q^{(0)}} + \dots + \frac{\tilde{p}^{(0)}}{\tilde{q}_{d+1} \|y\|^{d+1} + q^{(0)}}. \end{aligned} \quad (\text{A.71})$$

Hence, (ii) is straightforward from the fact that, for all  $s \in \{0, \dots, d\}$  and for all  $c > 0$  there exist  $a_s, b_s > 0$  such that

$$\frac{t^s}{t^{d+1} + c} \leq \frac{a_s}{t + b_s} \quad (\text{A.72})$$

for all  $t \geq 0$ . The proof of (iii) is analogous to the one of (ii).  $\square$

## References

- [1] Bardsley, J. M. and Goldes, J. (2009). Regularization parameter selection methods for ill-posed Poisson maximum likelihood estimation. *Inverse Problems*, 25(9):095005.
- [2] Benvenuto, F. (2017). A study on regularization for discrete inverse problems with model-dependent noise. *SIAM Journal on Numerical Analysis*, 55(5):2187–2203.
- [3] Benvenuto, F. and Campi, C. (2019). A discrepancy principle for the Landweber iteration based on risk minimization. *Applied Mathematics Letters*, 96:1–6.
- [4] Benvenuto, F. and Ferrari, A. (2010). Joint myopic deconvolution. *Inverse problems*, 26(10):105011.
- [5] Benvenuto, F., Haddar, H., and Lantz, B. (2016). A robust inversion method according to a new notion of regularization for Poisson data with an application to nanoparticle volume determination. *SIAM Journal on Applied Mathematics*, 76(1):276–292.
- [6] Benvenuto, F. and Jin, B. (2020). A parameter choice rule for Tikhonov regularization based on predictive risk. *Inverse Problems*.
- [7] Benvenuto, F. and Piana, M. (2014). Regularization of multiplicative iterative algorithms with nonnegative constraint. *Inverse Problems*, 30(3):035012.
- [8] Benvenuto, F., Schwartz, R., Piana, M., and Massone, A. M. (2013). Expectation maximization for hard X-ray count modulation profiles. *Astronomy & Astrophysics*, 555:A61.

- [9] Berger, J. O. (2013). *Statistical decision theory and Bayesian analysis*. Springer Science & Business Media.
- [10] Bertero, M. and Boccacci, P. (1998). *Introduction to inverse problems in imaging*. CRC press.
- [11] Bertero, M., Boccacci, P., and Ruggiero, V. (2018). *Inverse imaging with Poisson data*. IOP Publishing, Bristol.
- [12] Bertero, M., Boccacci, P., Talenti, G., Zanella, R., and Zanni, L. (2010). A discrepancy principle for Poisson data. *Inverse Problems*, 26(10):105004.
- [13] Bertero, M., De Mol, C., and Pike, E. R. (1985). Linear inverse problems with discrete data. i. general formulation and singular system analysis. *Inverse Problems*, 1(4):301–330.
- [14] Bertero, M., Lantéri, H., Zanni, L., et al. (2008). Iterative image reconstruction: a point of view. *Mathematical Methods in Biomedical Imaging and Intensity-Modulated Radiation Therapy (IMRT)*, 7:37–63.
- [15] Bissantz, N., Mair, B. A., and Munk, A. (2008). A statistical stopping rule for MLEM reconstructions in PET. In *2008 IEEE Nuclear Science Symposium Conference Record*, pages 4198–4200. IEEE.
- [16] Colton, D. and Kress, R. (2019). *Inverse acoustic and electromagnetic scattering theory*, volume 93. Springer Nature.
- [17] Deledalle, C.-A. (2017). Estimation of Kullback-Leibler losses for noisy recovery problems within the exponential family. *Electron. J. Statist.*, 11(2):3141–3164.
- [18] Deledalle, C.-A., Vaiteer, S., Fadili, J., and Peyré, G. (2014). Stein Unbiased GrAdient estimator of the Risk (SUGAR) for multiple parameter selection. *SIAM Journal on Imaging Sciences*, 7(4):2448–2487.
- [19] Dempster, A. P., Laird, N. M., and Rubin, D. B. (1977). Maximum likelihood from incomplete data via the EM algorithm. *Journal of the Royal Statistical Society: Series B (Methodological)*, 39(1):1–22.
- [20] Engl, H. W., Hanke, M., and Neubauer, A. (1996). *Regularization of inverse problems*, volume 375. Springer Science & Business Media.
- [21] Evans, S. N. and Stark, P. B. (2002). Inverse problems as statistics. *Inverse Problems*, 18(4):R55–R97.
- [22] Hohage, T. and Werner, F. (2016). Inverse problems with Poisson data: statistical regularization theory, applications and algorithms. *Inverse Problems*, 32(9):093001.
- [23] Hudson, H. M. (1978). A natural identity for exponential families with applications in multiparameter estimation. *The Annals of Statistics*, 6(3):473–484.
- [24] Johnson, N. L., Kemp, A. W., and Kotz, S. (2005). *Univariate discrete distributions*, volume 444. John Wiley & Sons.
- [25] Li, H., Werner, F., et al. (2020). Empirical risk minimization as parameter choice rule for general linear regularization methods. *Annales de l’Institut Henri Poincaré, Probabilités et Statistiques*, 56(1):405–427.

- [26] Llacer, J. and Veklerov, E. (1991). The use of a stopping rule in iterative image reconstruction. *Lecture Notes-Monograph Series*, pages 209–226.
- [27] Lucka, F., Proksch, T., Brune, C., Bissantz, N., Burger, M., Dette, H., and Wubbeeling, F. (2018). Risk estimators for choosing regularization parameters in ill-posed problems-properties and limitations. *Inverse Problems and Imaging*, 12(5):1121–1155.
- [28] Lucy, L. B. (1974). An iterative technique for the rectification of observed distributions. *The astronomical journal*, 79:745.
- [29] Massa, P., Piana, M., Massone, A. M., and Benvenuto, F. (2019). Count-based imaging model for the Spectrometer/Telescope for Imaging X-rays (STIX) in Solar Orbiter. *Astronomy & Astrophysics*, 624:A130.
- [30] Munk, A. and Pricop, M. (2010). On the self-regularization property of the EM algorithm for Poisson inverse problems. In *Statistical modelling and regression structures*, pages 431–448. Springer.
- [31] Politte, D. G. and Snyder, D. L. (1991). Corrections for accidental coincidences and attenuation in maximum-likelihood image reconstruction for positron-emission tomography. *IEEE Transactions on Medical Imaging*, 10(1):82–89.
- [32] Pouchol, C. and Verdier, O. (2020). The ML–EM algorithm in continuum: sparse measure solutions. *Inverse Problems*, 36(3):035013.
- [33] Ramani, S., Blu, T., and Unser, M. (2008). Monte-Carlo SURE: A black-box optimization of regularization parameters for general denoising algorithms. *IEEE Transactions on image processing*, 17(9):1540–1554.
- [34] Resmerita, E., Engl, H. W., and Iusem, A. N. (2007). The expectation-maximization algorithm for ill-posed integral equations: a convergence analysis. *Inverse Problems*, 23(6):2575–2588.
- [35] Richardson, W. H. (1972). Bayesian-based iterative method of image restoration. *JoSA*, 62(1):55–59.
- [36] Santos, R. J. and De Pierro, A. R. (2009). A new parameters choice method for ill-posed problems with Poisson data and its application to emission tomographic imaging. *International Journal of Tomography and Statistics*, 11:33–52.
- [37] Shepp, L. A. and Vardi, Y. (1982). Maximum likelihood reconstruction for emission tomography. *IEEE transactions on medical imaging*, 1(2):113–122.
- [38] Snyder, D. L., Hammoud, A. M., and White, R. L. (1993). Image recovery from data acquired with a charge-coupled-device camera. *J. Opt. Soc. Am. A*, 10(5):1014–1023.
- [39] Stein, C. M. (1981). Estimation of the mean of a multivariate normal distribution. *The annals of Statistics*, pages 1135–1151.
- [40] Zanella, R., Boccacci, P., Zanni, L., and Bertero, M. (2013). Corrigendum: efficient gradient projection methods for edge-preserving removal of Poisson noise. *Inverse Problems*, 29(11):119501.